THE EUROPEAN ENERGY RESEARCH ALLIANCE
DESIGN TOOLS FOR OFFSHORE WIND FARM CLUSTER

Validation of wake models for (two) wind farms

Kurt S. Hansen, Charlotte Hasager

December 2014

D 5.9

Agreement n.:	FP7-ENERGY-2011-1/ n°282797
Duration	January 2012 to June 2015
Co-ordinator:	DTU Wind Energy, Risø Campus, Denmark

Support by:

SEVENTH FRAMEWORK PROGRAMME

Document information

Document Name:	Validation of wake models for (two) wind farms
Document Number:	D 5.9
Author:	Kurt S. Hansen & Charlotte Hasager
Date:	December 2014
WP:	5
Task:	5.9

1 EXECUTIVE SUMMARY

The cluster performance, defined as the wake effect between two wind farms has been simulated and validated. This is the first benchmark on multiple wind farms, modelling the large-scale effects of more than 150 wind turbines. The validation has been performed on two large wind farms, separated with a distance of 33 diameters. The upwind wind farm consists of wind turbines installed on straight rows with a spacing of 11D, while the downwind wind turbines are located on arch's with variable spacing between 5-7 D. The sideways displacement of the wind farms is approximately 10D, which limits the inflow sector with visible cluster effects. SCADA data, recorded on the downstream wind farm, has been used to identify flow cases with visible clustering effects. The inflow condition is derived from a partly undisturbed wind turbine, due to lack of mast measurements.

The SCADA analysis conclude that centre of the deficit for a wind farm with variable spacing and undisturbed inflow is located 80-90 diameters downstream from the inflow turbines. Furthermore, the location of the deficit zone is not very sensitive to the inflow direction and the maximum deficit inside the zone is 20 – 25 %.

The analysis of disturbed inflow concludes that the maximum deficit zone is distinct and located only 5-10D downstream from the inlet. The size of the deficit zone increases and moves downstream for increasing inflow direction e.g. where the wind farm operates in partly wake conditions.

The eight models in the benchmark includes both RANS models, mesoscale models and engineering models. The flow cases, identified with wind speed and sector, have been simulated and validated towards the SCADA results. The validation confirms that a distinct triangular deficit zone appears 5-10D into the wind farm, when the wake encompass the downwind wind farm. The deficit zone, representing 20-30% speed reduction, increases and moves downstream for increasing inflow direction (partial cluster effect), and the external wake effect disappears outside a flow sector of ±15°.

The benchmark demonstrates that most the models are able to predict the cluster performance.

2 TABLE OF CONTENTS

1 EXECUTIVE SUMMARY 4

2 TABLE OF CONTENTS 5

3 INTRODUCTION 6

3.1 Wake models participating in the EERA-DTOC wind farm cluster benchmark 6
3.2 Identification of flow cases 7
3.3 Quality of SCADA measurements 8

4 PRESENTATION OF MODEL RESULTS 9

4.1 Case westerly inflow 9
4.2 Case easterly inflow 11
4.3 Easterly clustering 12

5 CONCLUSION 13

6 REFERENCES 14

7 ANNEX A: WESTERN INFLOW DIRECTION 15

7.1 CASE: RS-270-7 15
7.2 Power deficit along arch's, RS-270-7 16
7.3 CASE: RS-275-7 17
7.4 Power deficit along arch's, RS-275-7 18
7.5 CASE RS-280-7 19
7.6 Power deficit along arch's, RS-280-7 20
7.7 CASE RS-285-7 21
7.8 Power deficit along arch's, RS-285-7 22
7.9 CASE RS-290-7 23
7.10 Power deficit along arch's, RS-290-7 24

8 ANNEX B - EASTERN INFLOW DIRECTION 25

8.1 Case RS-77-8. 25
8.2 Power deficit along arch's, RS-77-8. 26
8.3 Case RS-87-8. 27
8.4 Power deficit along arch's, RS-87-8 28
8.5 Case RS-97-8. 29
8.6 Power deficit along arch's, RS-97-8 30
8.7 Case RS-107-8. 31
8.8 Power deficit along arch's, RS-107-8 32
8.9 Case RS-117-8. 33
8.10 Power deficit along arch's, RS-117-8 34

9 ANNEX C - CLUSTER EFFECT FOR EASTERLY INFLOW; 35

9.1 Case NY & RS-77-8 35
9.2 Case NY & RS-87-8 36
9.3 Case NY & RS-97-8 37
9.4 Case NY & RS-107-8 38
9.5 Case NY & RS-117-8 40

3 INTRODUCTION

The benchmark of the wake models applied to (two) nearby wind farms have been concluded. The two wind farms are 1) Rødsand II (RS) offshore wind farm, consisting of 90 wind turbines and 2) Nysted (NY) offshore wind farm consisting of 72 wind turbines as described in [1] and visualized in Figure 1. Both wind farms are located in Femern Belt, which is the entrance to the Baltic Sea, south of Denmark

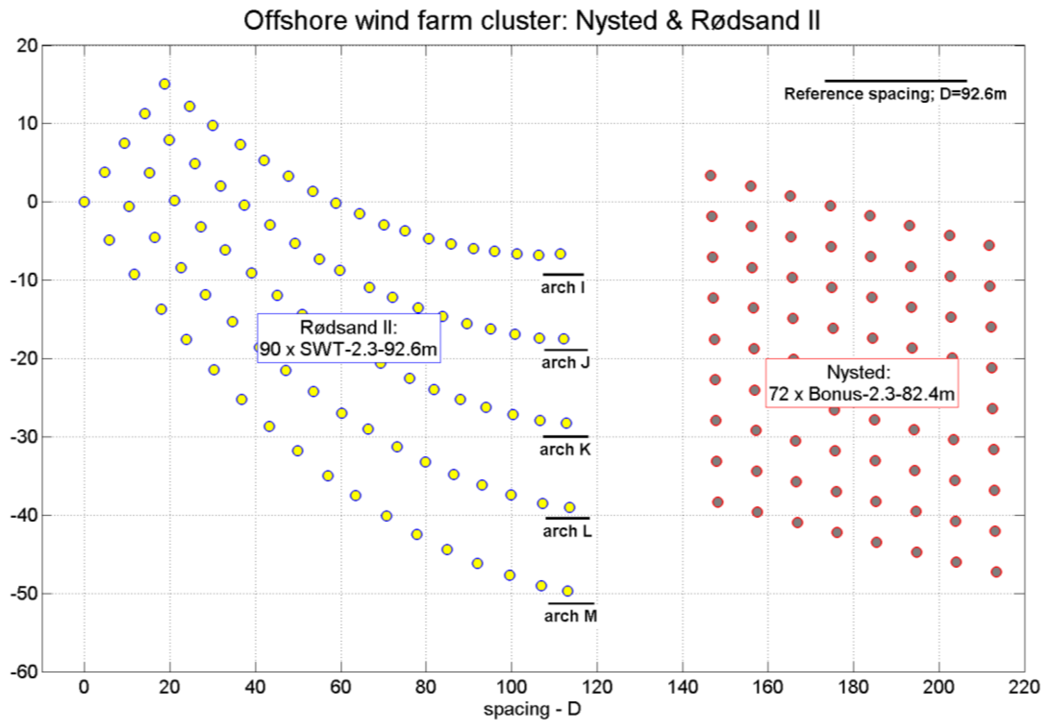

Figure 1: Offshore wind farm cluster consisting of the Rødsand II and Nysted wind farms.

The flow cases listed in Figure 2 represents two main wind directions:

i) Westerly wind (270 - 290°) and
ii) Easterly wind (77- 117°).

As illustrated in Figure 2.

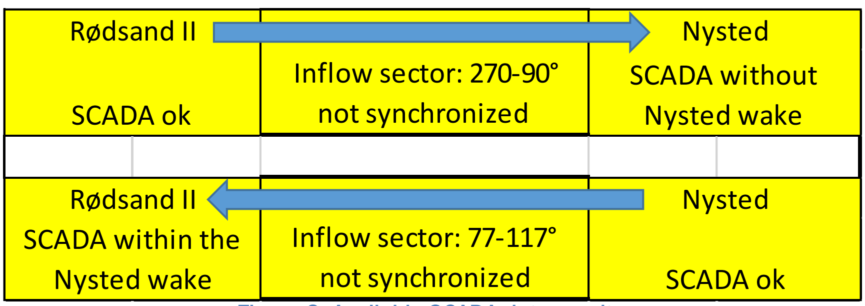

Figure 2: Available SCADA data results.

3.1 Wake models participating in the EERA-DTOC wind farm cluster benchmark

The combined flow cases have been simulated with nine different models, as listed inTable 1: Wake models participating in the EERA-DTOC wind farm cluster benchmark.
Rødsand II wind farm have been simulated by most of the participants both for western and eastern directions, while the Nysted wind farm has only been simulated for the eastern wind direction with three models according to Table 2: Simulation matrix for the cluster benchmark.. Based on Table 1 it is possible to verify and validate:

I) Flow through Rødsand II WF, westerly inflow;
II) Flow through Nysted WF, easterly inflow;
III) The cluster effect for easterly inflow.

Although we do not have access to synchronized SCADA representing both Rødsand II and Nysted wind farms.

Table 1: Wake models participating in the EERA-DTOC wind farm cluster benchmark.

	SCADA(BA)	DTU Wind Energy/KSH	kuhan@dtu.dk
1	AD/RANS	UPORTO/Palma	jpalma@fe.up.pt
2	CFDWake	CENER/B.Hevia	bgarcia@cener.com
3	CRESflowNS	CRES/ John Prop.	jprosp@cres.gr
4	FarmFlow	ECN Wind Energy/Scheepers	schepers@ecn.nl
5	FUGA/SO	DTU Wind Energy/S.Ott	sqot@dtu.dk
6	NOJ(GU)	DTU Wind Energy/A.Pena	aldi@dtu.dk
7	NOJ/Penã	DTU Wind Energy/A.Pena	aldi@dtu.dk
8	WRF/UPM	Ciemat/Ana.Palomares	ana.palomares@ciemat.es
9	Meso/PV	DTU Wind Energy/P.Volker	pvol@dtu.dk

Table 2: Simulation matrix for the cluster benchmark.

EERA-DTOC		Rødsand II		Nysted	
Institution/Models		RS; 270-290°	RS; 77-117°	NY; 270-290°	NY; 77-117°
DTU	SCADA(BA)	15	13	20	15
CRES	CRESflowNS	15	-	-	-
UPORTO	AD/RANS	10	9	-	9
ECN	FarmFlow	20	15	-	15
DTU	NOJ/Penã	15	15	-	-
DTU	NOJ(GU)	15	15	-	-
DTU	FUGA/SO	-	15	-	-
Ciemat	WRF/UPM	18	12		6
CENER	CFDWake	4	-	-	-
Scada data recorded before installation of Rødsand II					
Rødsand II is operating in the wake of Nysted					

3.2 Identification of flow cases

The total number includes 55 flow cases for Rødsand II wind farm and Nysted wind farm as listed in Table 3. The flow cases are derived from the limited amount of SCADA data, recorded during one month where U=5 & 11 m/s are weakly represented.

Table 3: Flow case simulation matrix - not prioritized.

		wind speed			
Western inflow:	Wind dir	U = 5 m/s	U = 7 m/s	U = 9 m/s	U = 11 m/s
RS & NY	270°	x	x	x	x
RS & NY	275°	x	x	x	x
RS & NY	280°	x	x	x	x
RS & NY	285°	x	x	x	x
RS & NY	290°	x	x	x	x
		wind speed			
Eastern inflow:	Wind dir	U = 6 m/s	U = 8 m/s	U = 10 m/s	
RS & NY	77°	x	x	x	
RS & NY	87°	x	x	x	
RS & NY	97°	x	x	x	
RS & NY	107°	x	x	x	
RS & NY	117°	x	x	x	

Flow case naming: RS_270_5 indicates simulation of all the Rødsand II wind turbines based on uniform inflow at 8 m/s from a flow sector of 270±2.5°.

3.3 Quality of SCADA measurements

The wind speed inside Rødsand II wind farm has been derived from the individual wind turbine power values, with reference to the official power curve. The official power curve has been measured at an ideal (flat) onshore location - without obstacles. None of the offshore wind turbine power curves have been validated. There can be a considerable deviation between onshore and offshore blade surface roughness due to the saline environment, which influences the power curve. Furthermore, the wind conditions will differ in terms of shear, turbulence and atmospheric stability. The wind speed at each wind turbine location has been derived directly from the power curve without taking into account the rotor speed and the pitch angle setting. It is not possible to determine the uncertainty of the derived wind speed due to lack of direct measurements.
For westerly wind direction, the front row e.g. I1, J1, K1, L1 & M1 has been used as reference wind turbines.
For easterly wind direction wind turbine M18 is used as reference for both wind speed a for easterly wind directions, despite this turbine is operating is partly in the wake of the Nysted wind farm.
The inflow wind speed for Nysted wind farm is measured at hub height on an undisturbed mast located either west or east of the wind farm – before the installation of Rødsand II wind farm.
The wind direction for Rødsand II wind farm have been derived from a group of reference wind turbines, based on the yaw position, which was calibrated according the deficit distribution combined with the wind turbine positions.
The wind speed values inside Nysted wind farm are derived from individual power values, combined with the official power curve. This turbine is active stall controlled, operating at two distinct rotor speeds, which will increase the uncertainty of the derived wind speed.

4 PRESENTATION OF MODEL RESULTS

Both SCADA and model results are provided as power values for each wind turbine in each of the two wind farms where the comparison is performed for the following parameters:

i) Distribution of normalized wind speed across the wind farms consisting of either 90 or 72 wind turbines;
ii) Power deficit along arch's of (18) wind turbines for Rødsand II;
iii) Model performance calculated as a comparison between model results and SCADA recordings using the Normalized Mean Absolute Error (NMAE) method (1).

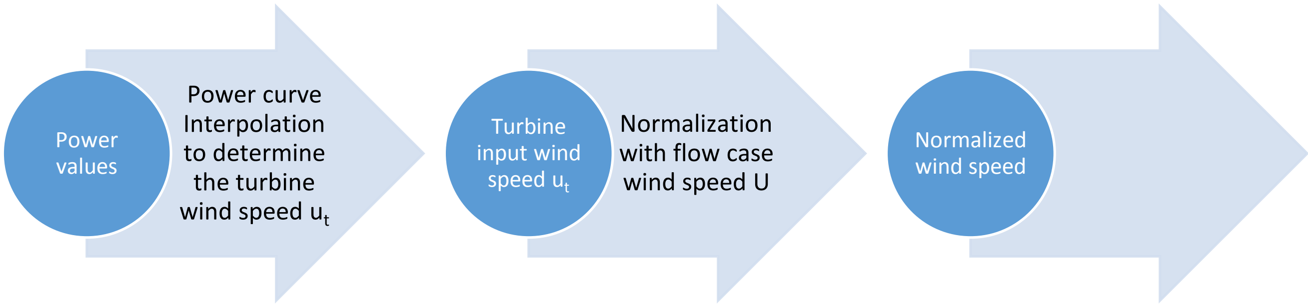

Figure 3: Process used to calculate the normalized wind speed.

The process for determining the normalized wind speed is shown in Figure 3. The official power curves for Bonus 2.3 MW and SWT 2.3-93 are used to determine the turbine wind speed u_t ; see reference [1], Annex F & G.
The flow case sector wind speed U is equal to the wind speed listed in Table 3.
NMAE is a statistical method, which has been introduced in IEA Task 31 WakeBench, [2]:

$$NMAE(\hat{\delta}_{ijk}) = \frac{1}{\delta_{ijk}^{obs} \cdot N_S} \sum_{s=1}^{N_s} \left| \hat{\delta}_{ijk,s}^{obs} - \hat{\delta}_{ijk,s}^{sim} \right|; \quad \hat{\delta}_{ijk} = \frac{\delta_{ijk}}{\delta_0} \qquad (1)$$

where $\hat{\delta}_{ijk}$ is the variable of interest made dimensionless by dividing by a reference value δ_0 that corresponds to the inflow wind speed, as prescribed in the benchmark.

4.1 Case westerly inflow

Westerly inflow includes only undisturbed inflow to Rødsand II wind farm for five distinct sectors: 270±2.5°, 275±2.5°, 280±2.5°, 285±2.5° and 290±2.5° in combination with four wind speed intervals: 5±0.5 m/s, 7±0.5 m/s, 9±0.5 m/s and 11±0.5 m/s. The model result for wind speed interval: 7±0.5 m/s has been visualized in Annex A.

1. Case: RS-270-7, section 5.1 has been simulated by 7 participant and the result seems to correlate well with the SCADA results, except that the predicted mixing results in a more distinct speed reduction at the wind farm outlet. The power deficits along the arch's, section 7.2, illustrates a good agreement. The deficit at the outlet indicates a larger variation; furthermore, the inflow along arch M is undisturbed uniform for all wind turbines. The qualification of the results (NMAE) are visualized on Figure 4a, where five models agrees well with the SCADA results.
2. Case: RS-275-7, section 5.3, has been simulated by 6 participants and the model predicts a higher wind speed reduction in the NE corner of the wind farm - compared to the SCADA data. The power deficits along the arch's, section 7.4, shows a good agreement downstream except for some scatter around 2-3 row, due to local wake conditions. The qualification of the results (NMAE) is visualized on Figure 4b, where four of the models agrees well with the SCADA data.
3. Case RS-280-7: section 5.5 has been simulated by five participants, here the model predicts a large wind speed reduction in the NE corner of the wind farm compared to the SCADA data. One model seems to have simulated the flow at a lower ambient wind speed. The predictions along the arch's, section 7.6, indicates a larger

downstream deficit. The qualification of the results (NMAE) is visualized on Figure 4c where all five models agrees quite well with the SCADA data.

4. Case RS-285-7, section 7.7 has been simulated by five participants. The majority of the models predict large speed reduction across the whole wind farm, 60 – 100D downstream. The power deficit along arch's, section 7.8, shows a large deficit. The qualification of results (NMAE) is visualized in Figure 4d where all models agrees well with the SCADA data.
5. Six participants has simulated Case RS-290-7, section 7.9 and predicts a large speed reduction across the whole wind farm compared to the SCADA data, 40 – 80D downstream. The power deficit along arch's, section 7.10, confirms the large deficit sector inside the wind farm 40-60D downstream. A comparison of model performance in Figure 4e displays how the models agree well with the SCADA data.

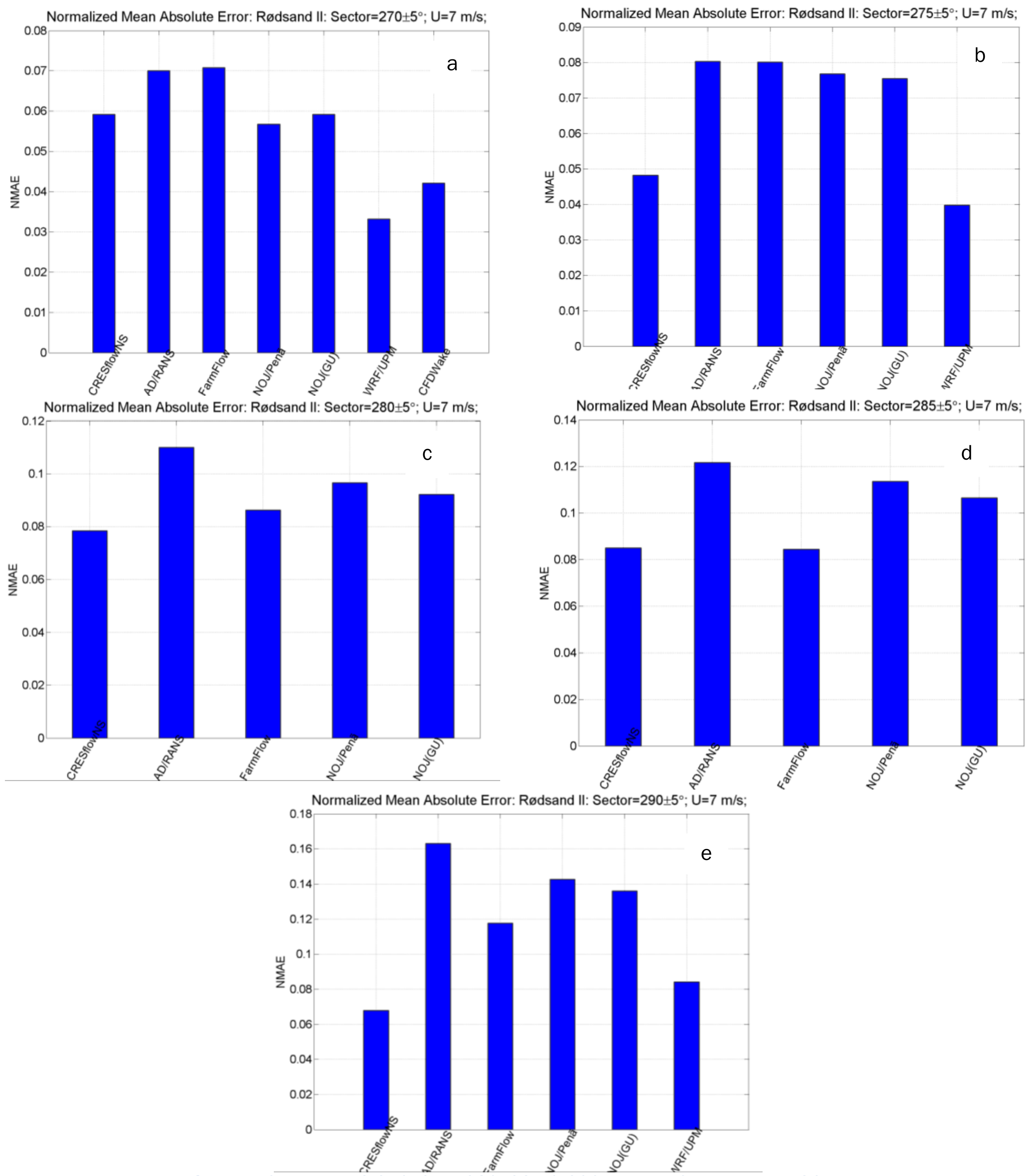

Figure 4: NMAE for cases RS-270, 275, 280, 285 & 290-7 with reference to the SCADA data.

4.2 Case easterly inflow

Easterly inflow includes disturbed inflow to Rødsand II wind farm for five distinct sectors: 77±5°, 87±5°, 97±5°, 107±5° and 117±5°in combination with three wind speed intervals: 6±0.5 m/s, 8±0.5 m/s and 10±0.5 m/s.
SCADA and model results for wind speed interval 8±0.5 m/s are visualized in Annex B. The whole wind farm is modelled as a single grid-cell in the Mesoscale model and the resulting wind speed is represented with a single value. The wind speed ratio is plotted with an appropriate colour for comparison reasons.
Note: due to lack of an undisturbed inflow reference, the comparison between SCADA and model results are problematic for sector 72-92° because the inflow reference is partly located in the wake. Some of the arch plots even shows negative deficit values due to a disturbed inflow reference value.

1. Case RS-77-8 in section 8.1 demonstrates that the model agrees well but predicts larger speed reduction compared to the SCADA results. The NMAE values for all models, except the Mesoscale model agrees well according to Figure 5a.
2. Case RS-87-8 in section 8.3 demonstrates good agreement, where most of the models predict the triangular speed reduction zone in the NE part of the WF, initiated by Nysted WF wake. This behaviour is also visible through the distinct increase in the power deficit between row 18 and row 17 in the arch plots, section 8.4. The NMAE values on Figure 5b present a high level of agreement for most of the models.
3. Case RS-97-8, viz. in section 8.5 demonstrates how the speed reduction zone or triangle moves downstream towards W for increasing inflow direction. The distinct increase of power deficit is moved towards S in arch's plots, section 8.6. All the models predicts well the deficit ant the NMAE bars, Figure 5c except for the Mesoscale model.
4. Case RS-107-8, viz. in section 8.7; most of the Nysted WF influence has disappeared, but some models predict a strong N-S area at 90D with a distinct and visible speed reduction. All models predict the increased speed around the SE WF "corner", with undisturbed inflow. This is visible in the arch plots, section 8.8 and reflected in the NMAE results on Figure 5d.
5. Case RS-107-8, viz. in section 8.9; where some of the models predicts a large distinct speed deficit area, centred around the 30D position. All models predict the increased speed around the SE WF "corner" with undisturbed inflow. The arch plot in section 8.10 together and the NMAE values in Figure 5e demonstrates a limited scatter compared to the previous sector results.

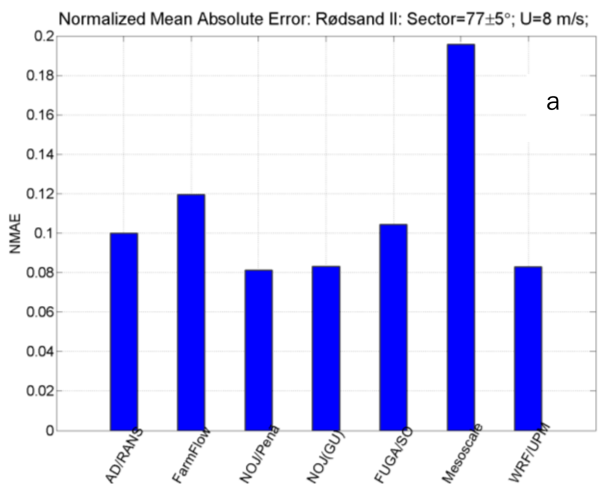

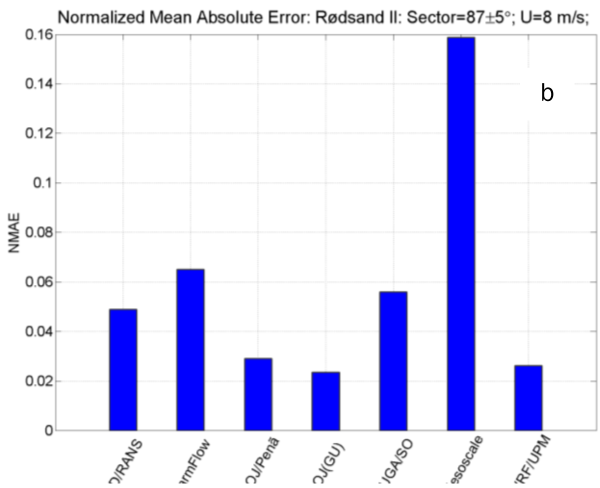

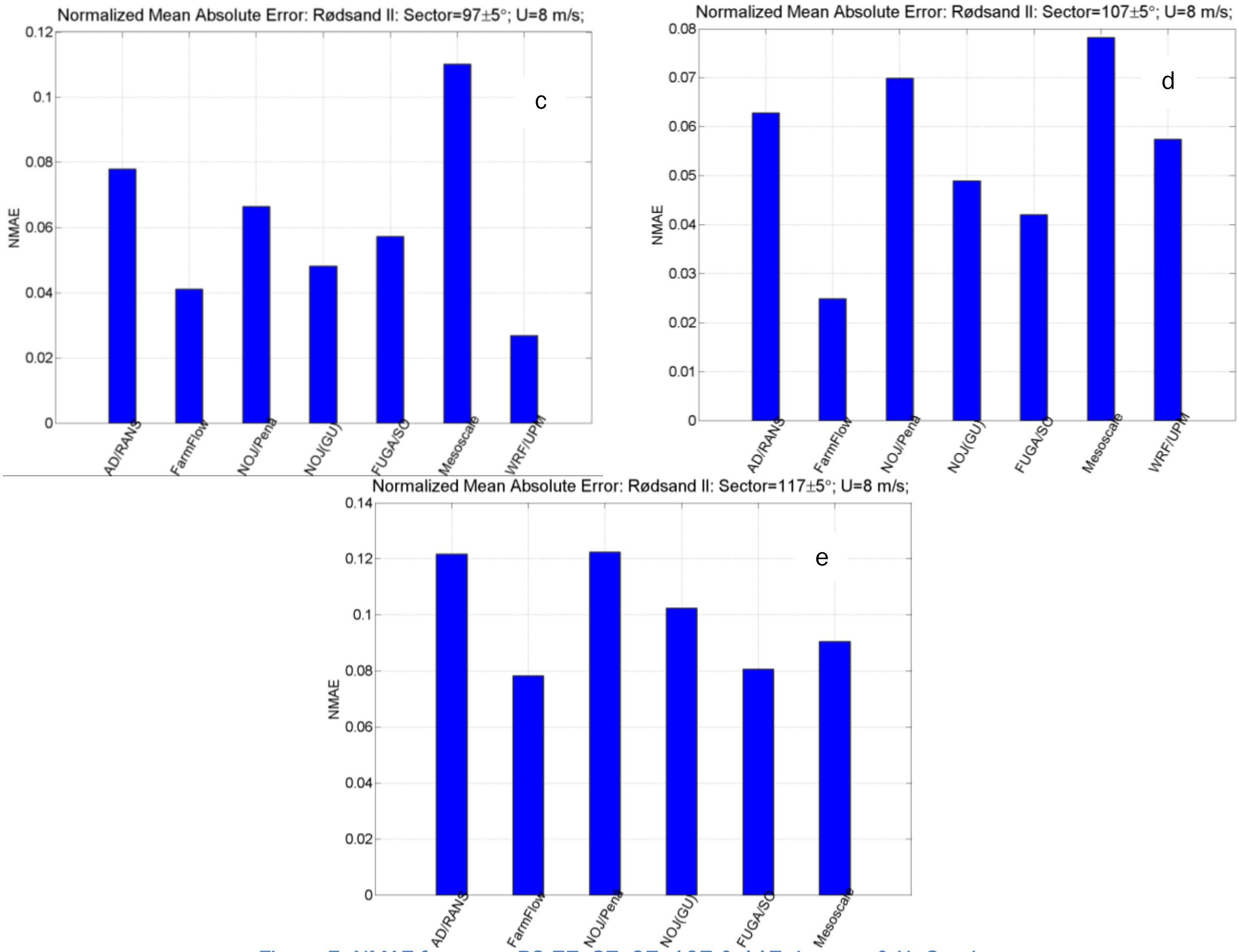

Figure 5: NMAE for cases RS-77, 87, 97, 107 & 117 degrees & U=8 m/s.

4.3 Easterly clustering

The combined effect of two wind farms is modeled for five distinct sectors: 77, 87, 97, 107 & 117±5° at 8 m/s and compared to SCADA results. The SCADA results for the two wind farms are not synchronised due to lack of information, while the Nysted (NY) SCADA dataset has been obtained before installation of the Rødsand II (RS) wind farm.
Comparison of the power distribution for the two wind farms is difficult, while the turbines are different. The official power curve for each wind turbine type have been used to re-calculate the inflow wind speed. The RS plots in this section have been addressed in the previous section and this section does not include a quantification of the results due lack of synchronization between the wind farms SCADA data.

1. Case NY & RS-77-8, viz. in section9.1, two models has simulated the cluster effect. Visually the model results agree well both for the Nysted and Rødsand II wind speed distribution.
2. Case NY & RS-87-8, viz. in section9.2, two models has simulated the cluster effect. Visually the model results agree well for the Nysted and Rødsand II wind speed distribution, but with a difference in the speed reduction in the Rødsand II WF. The “triangular” deficit zone behind the first row of turbines are visible both from SCADA and predictions.
3. Case NY & RS-97-8, viz. in section9.3, the Nysted wind farm demonstrates maximum deficit when the flow sector is centred along the EW NY rows. Both models captures the cluster effect, which is located at 90D in the Rødsand wind farm. Visually the model and SCADA results agree well.
4. Case NY & RS-107-8, viz. in section 9.4, has been simulated with three models. All models predicts the wind speed distribution in Nysted and Rødsand II wind farms well compared to the SCADA data. The distinct deficit zone has moved downstream, to 60D location for this inflow direction.
5. Case NY & RS-107-8, viz. in section 9.5 has been simulated by two models and for this direction the Nysted WAKE is only slightly visible in the NE corner of the Rødsand II WF. The distinct predicted deficit zone has moved further downwards to 30D but is not visible in the SCADA data anymore.

5 CONCLUSION

The benchmark demonstrates a good model agreement for flow simulation in wind farms with variable spacing. Both size and location of the distinct deficit zone caused by the Nysted wind farm is predicted well by the different models.

6 REFERENCES

[1] D 5.6 Production data from (two) operating wind farms, June 2014, EERA DTOC report.

[2] IEA-Task 31 WAKEBENCH: *Towards a protocol for wind farm flow model evaluation*. *Part 2: Wind farm wake models* by P.Moriarty et.al. presented Torque2014, available from Journal of Physics: Conference Series 524 (2014) 012185 doi:10.1088/1742-6596/524/1/012185.

7 ANNEX A: WESTERN INFLOW DIRECTION

7.1 CASE: RS-270-7

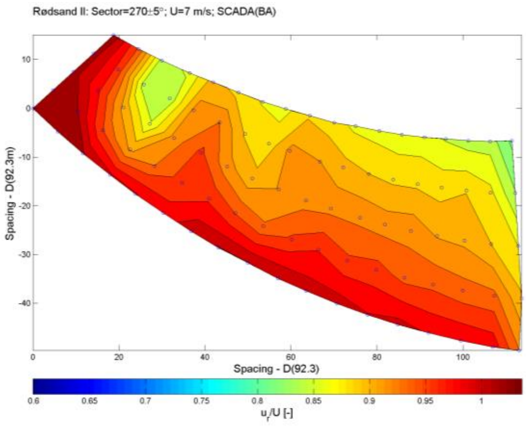

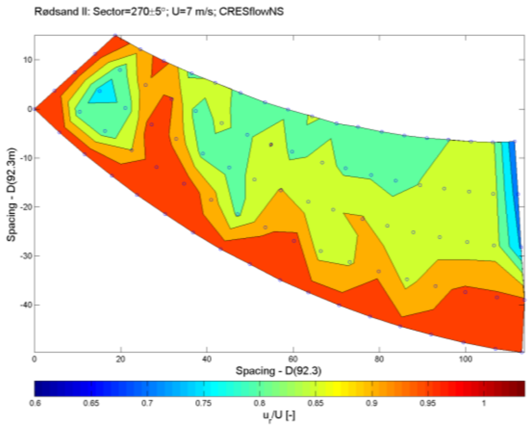

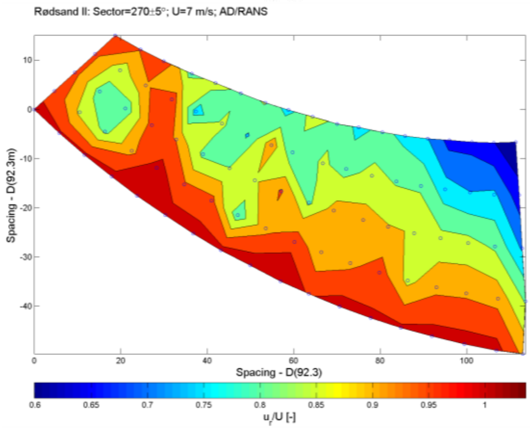

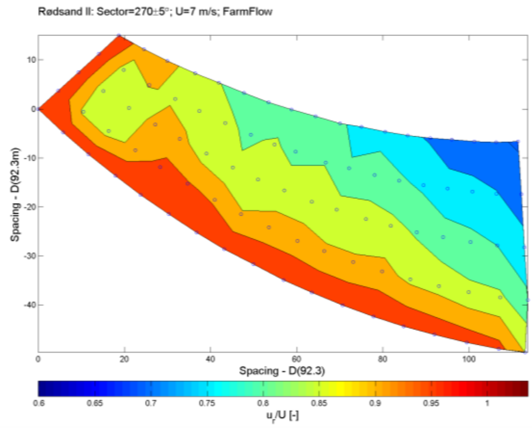

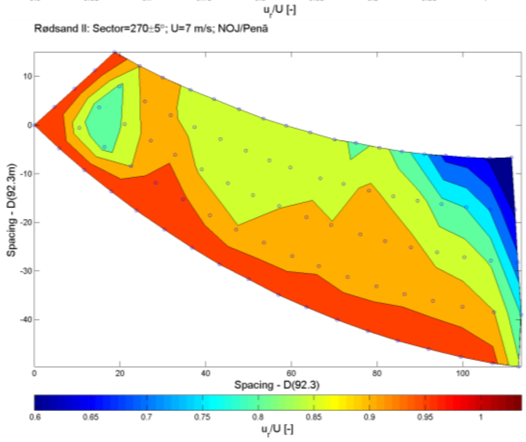

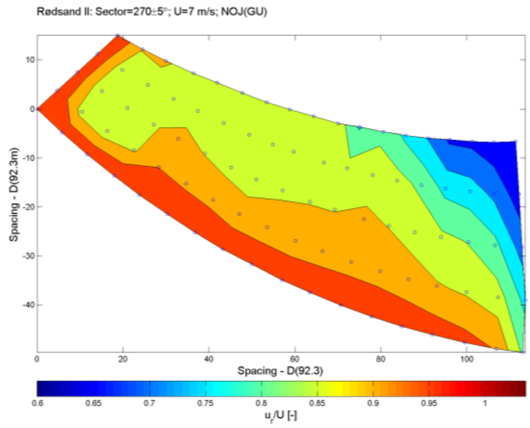

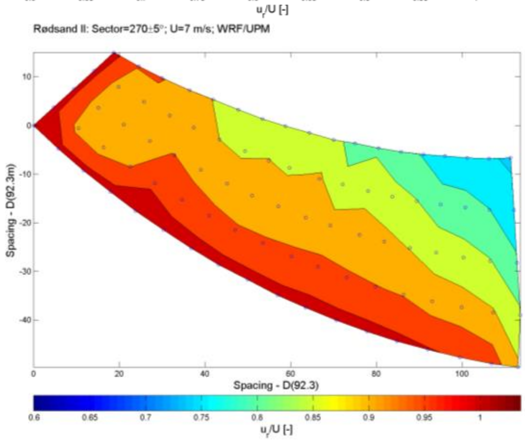

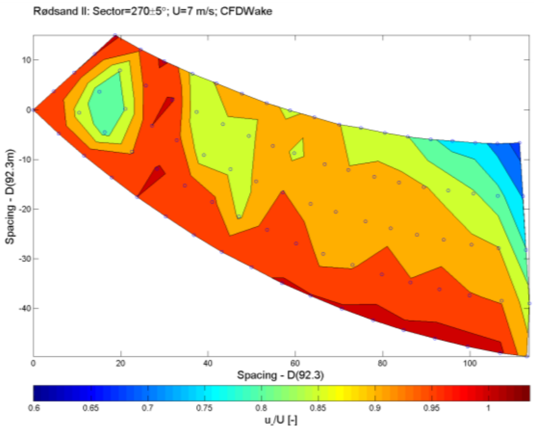

7.2 Power deficit along arch's, RS-270-7.

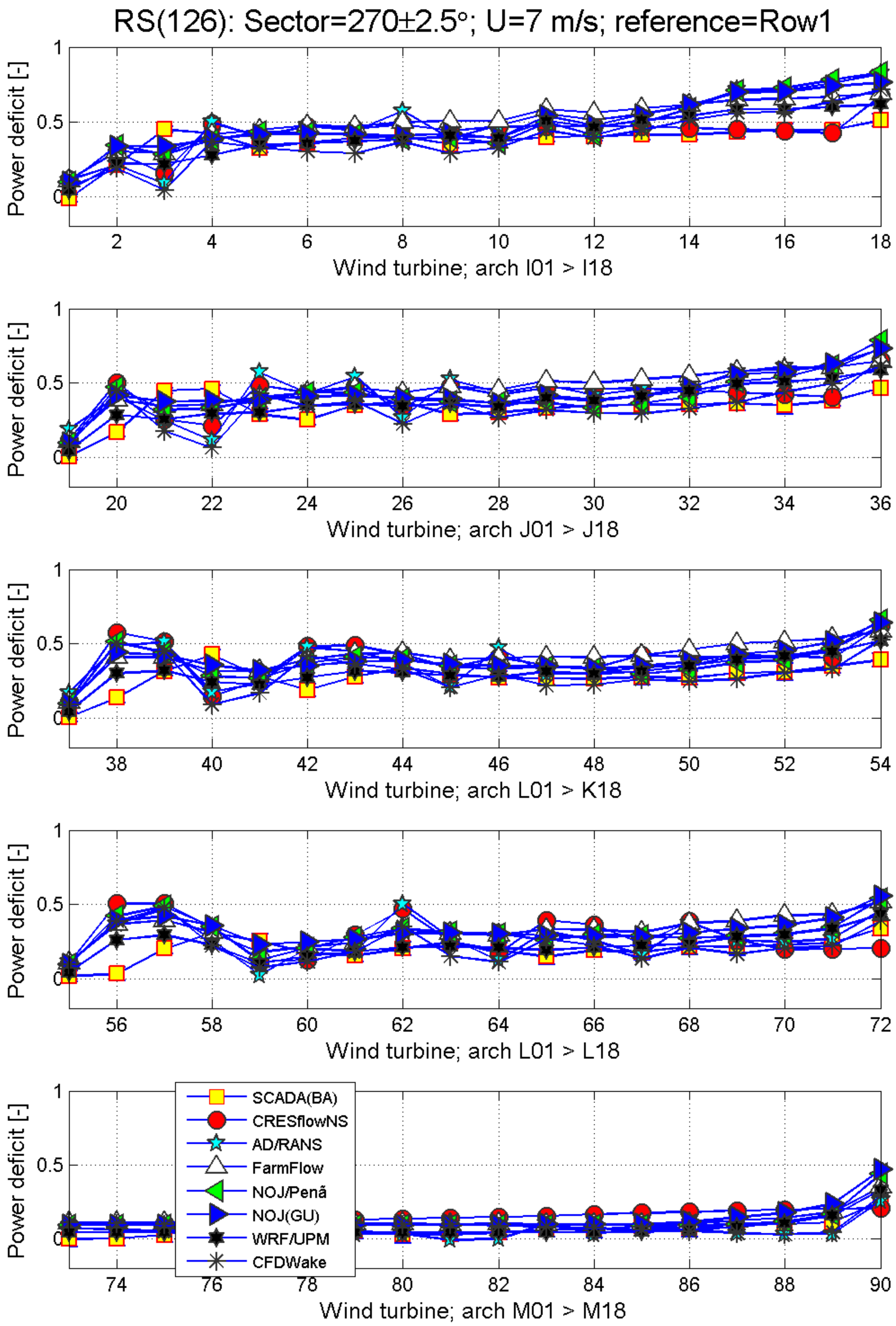

7.3 CASE: RS-275-7

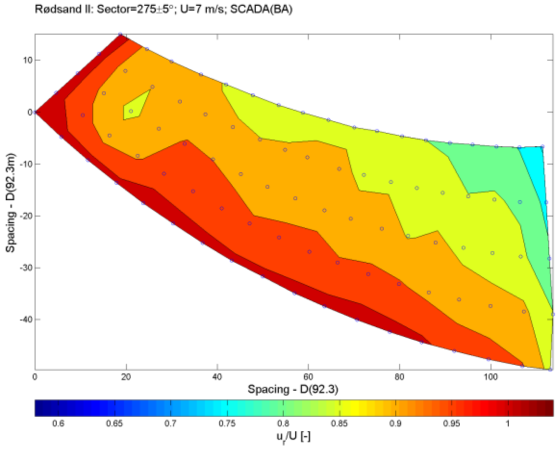

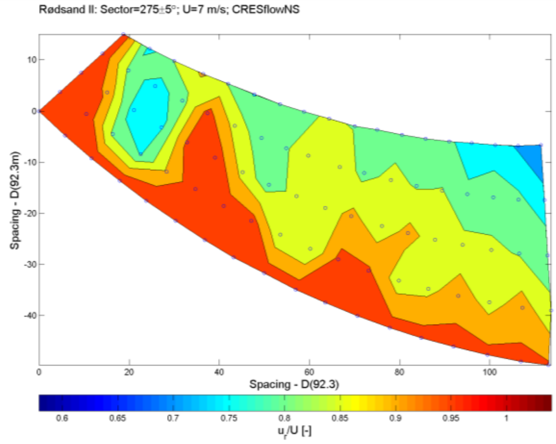

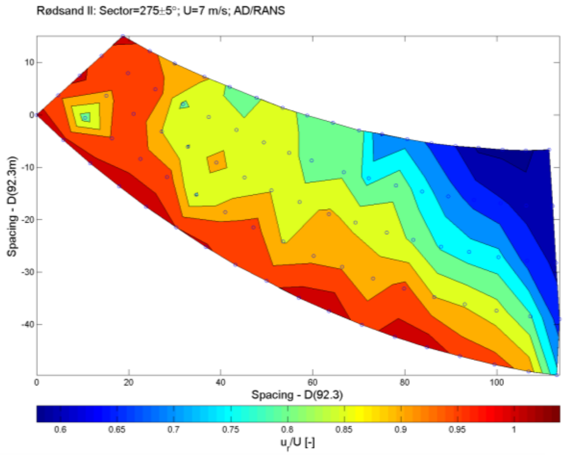

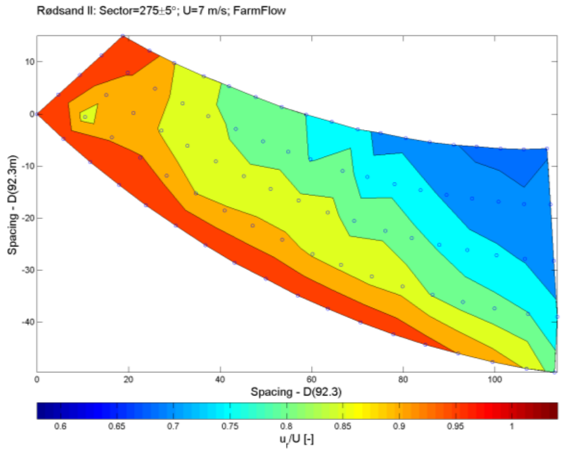

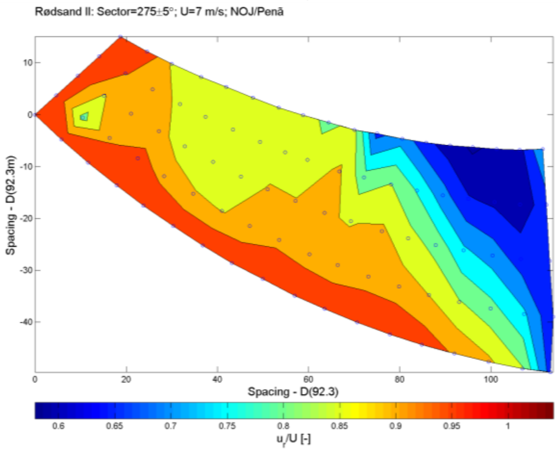

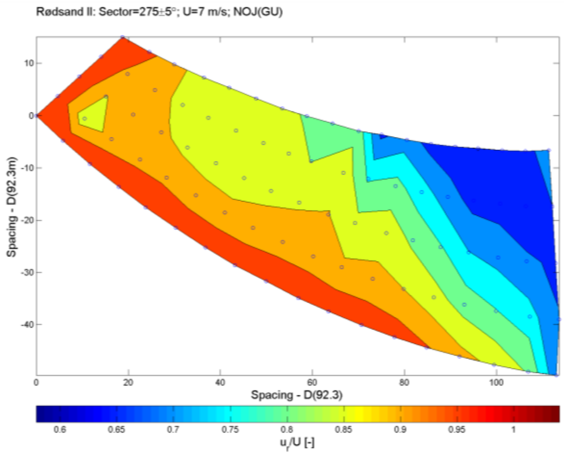

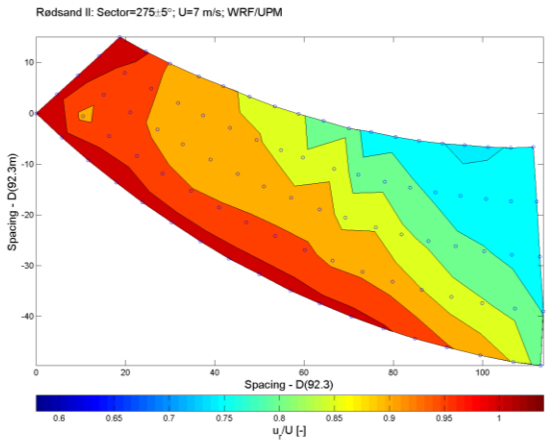

7.4 Power deficit along arch's, RS-275-7.

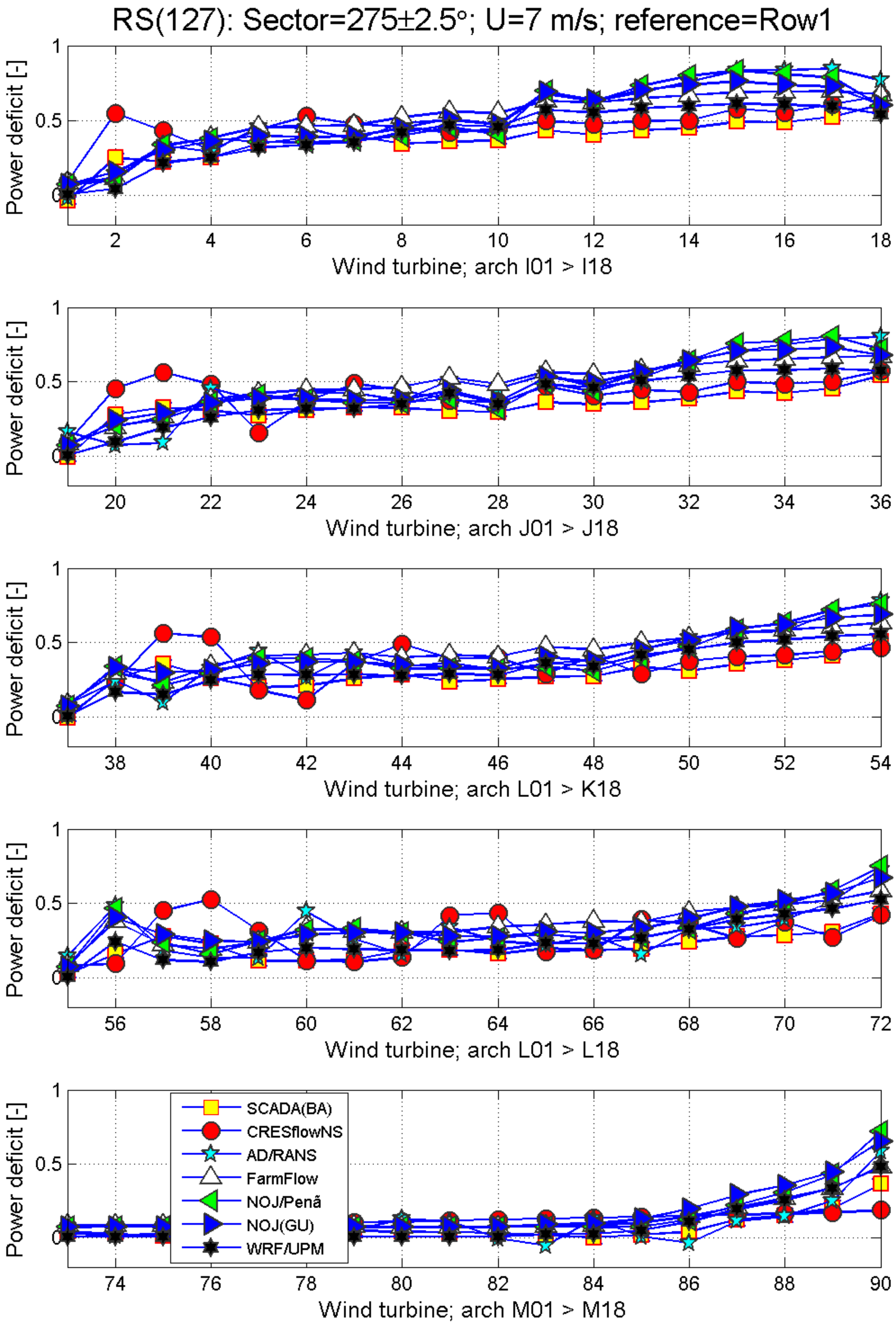

7.5 CASE RS-280-7.

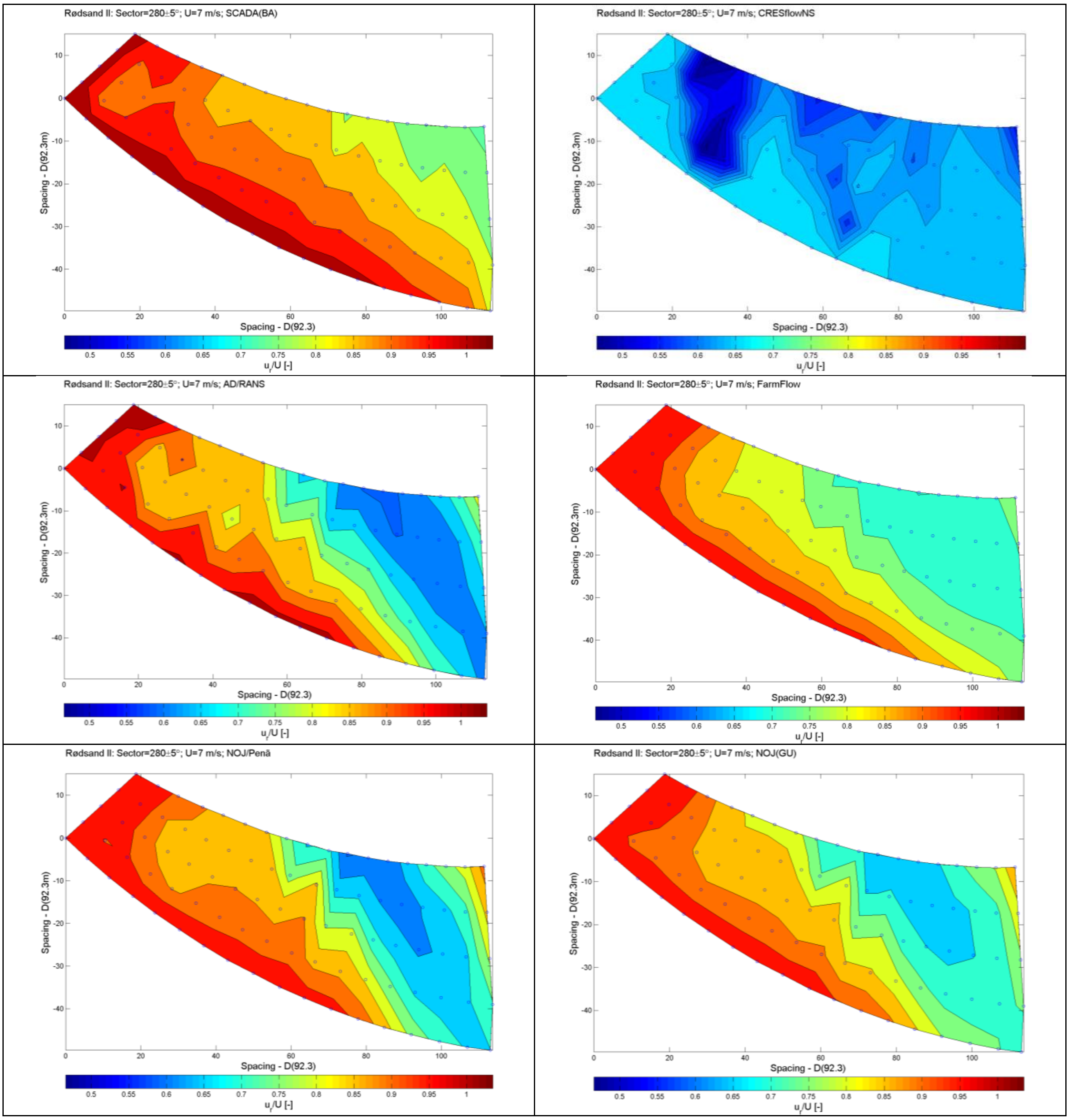

7.6 Power deficit along arch's, RS-280-7.

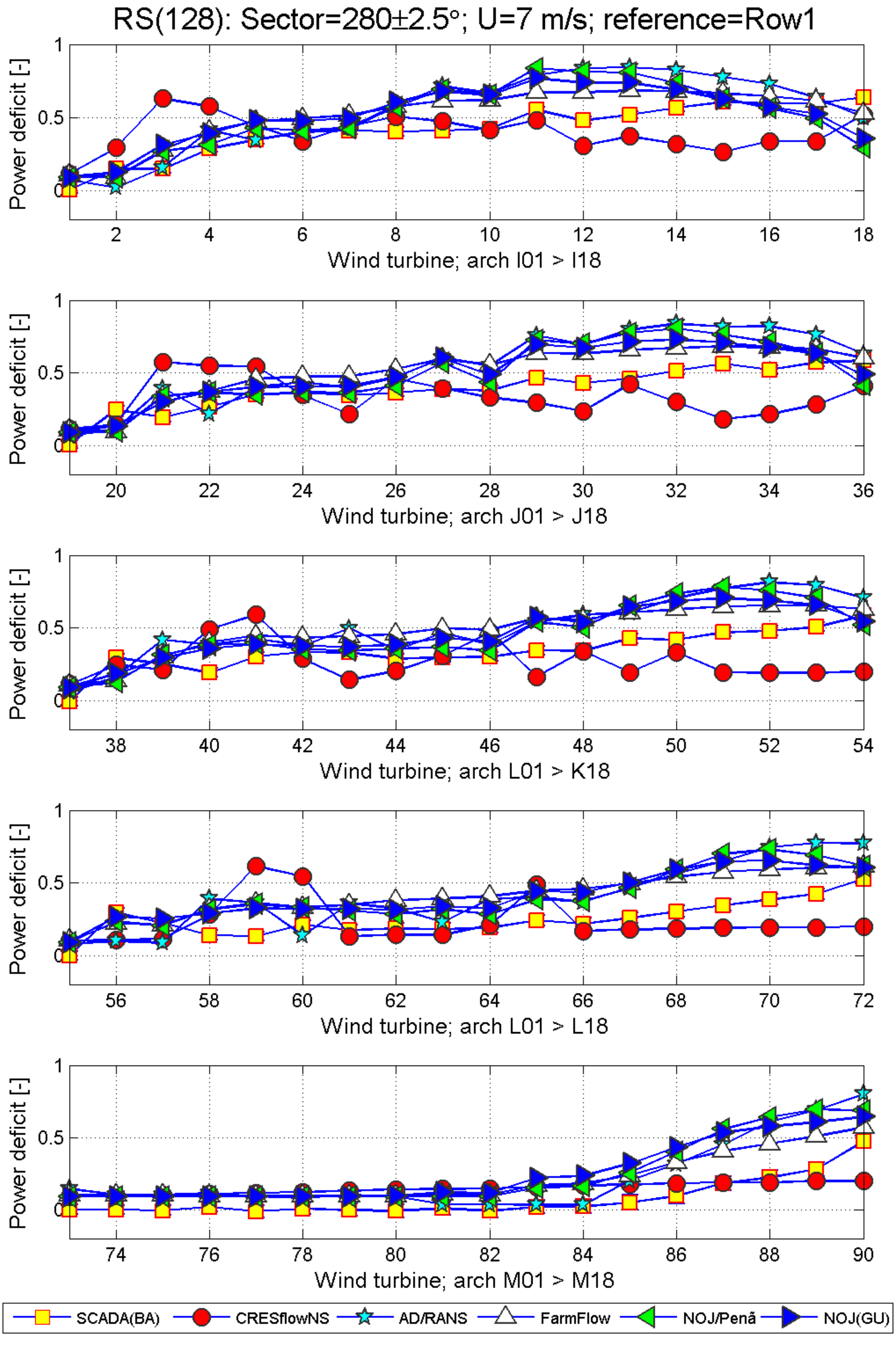

7.7 CASE RS-285-7.

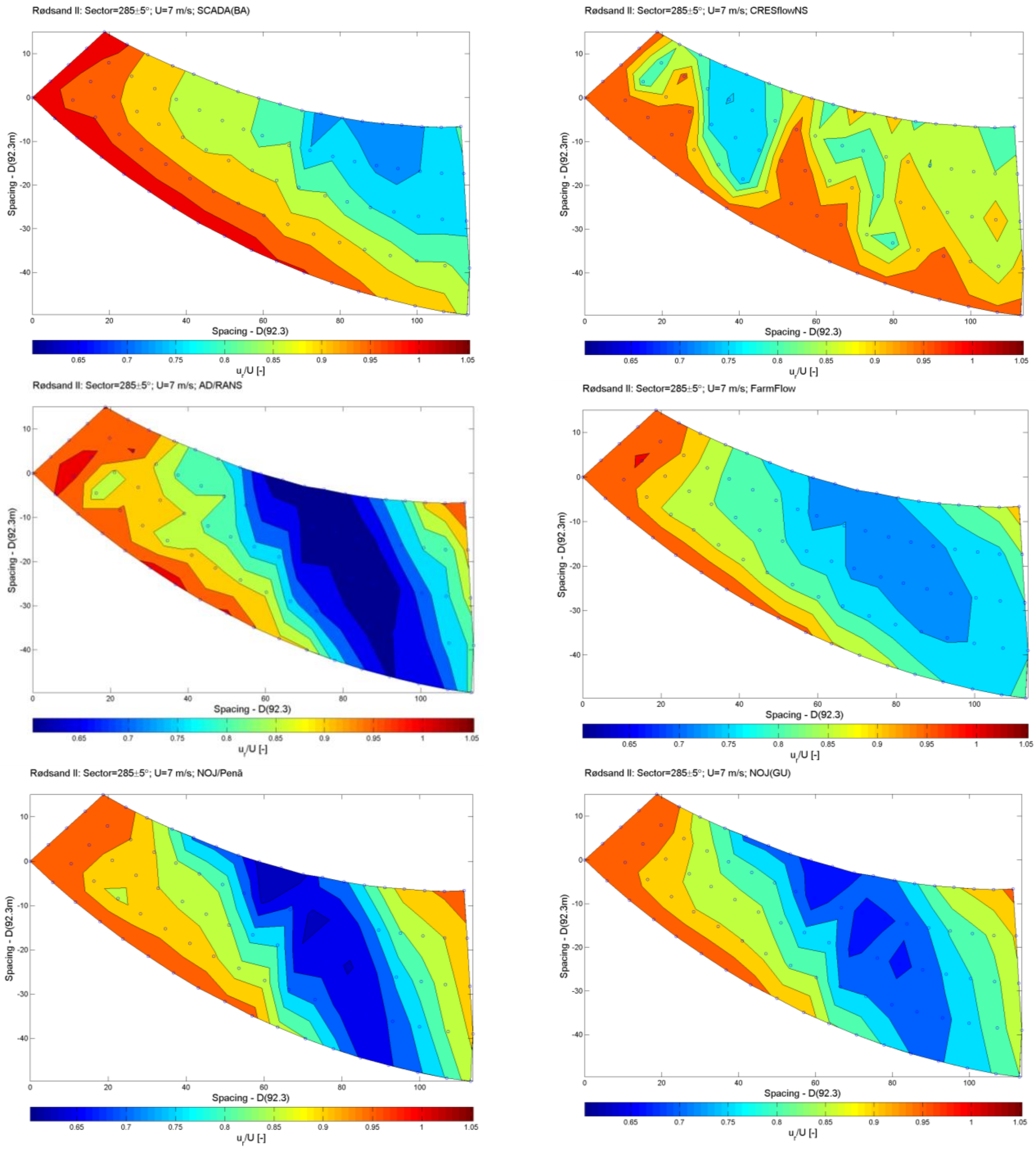

7.8 Power deficit along arch's, RS-285-7.

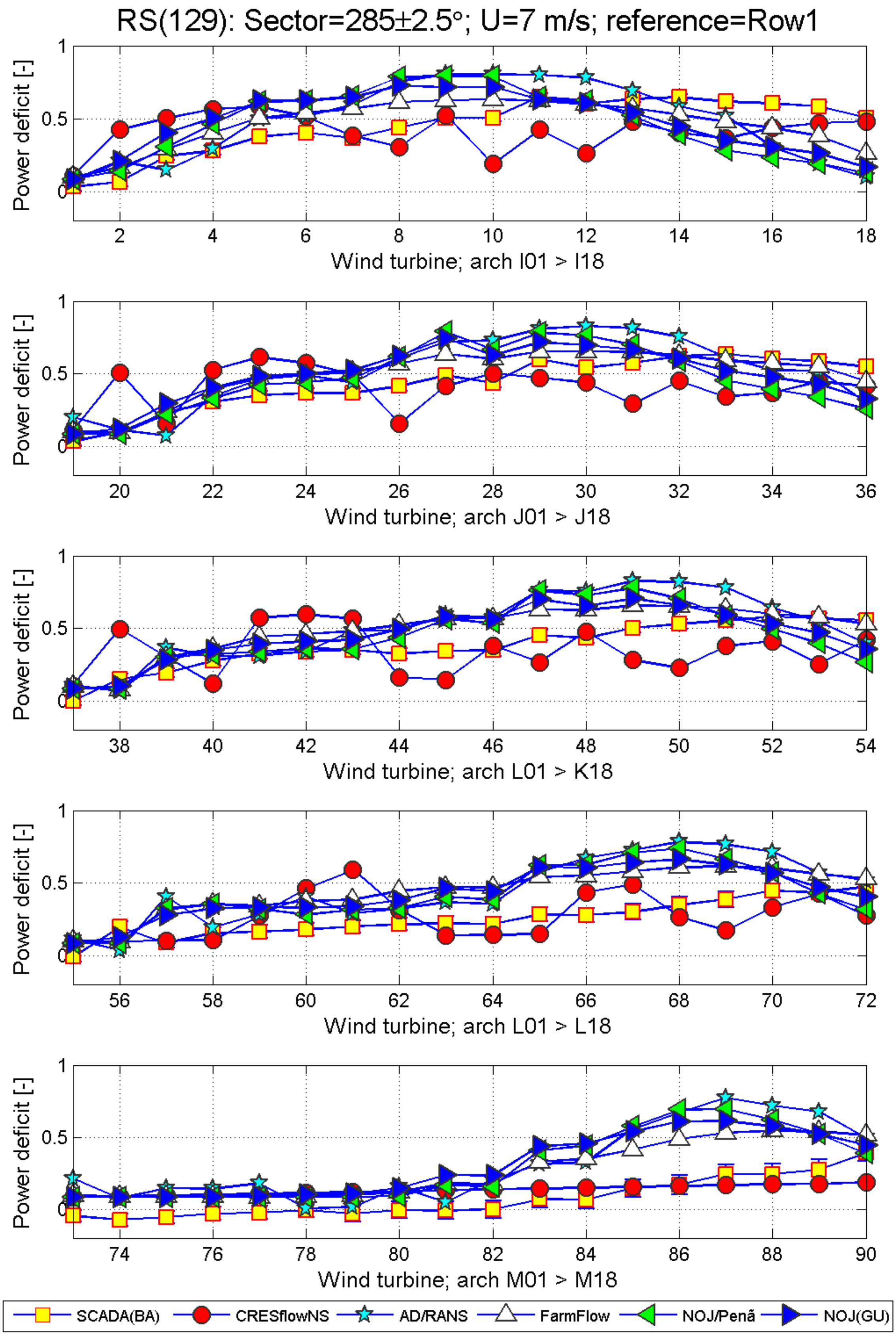

7.9 CASE RS-290-7.

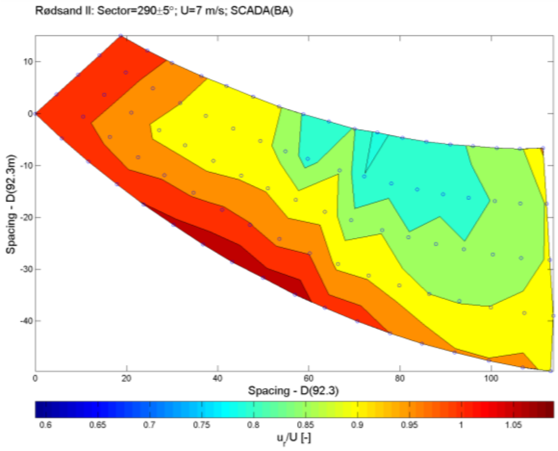

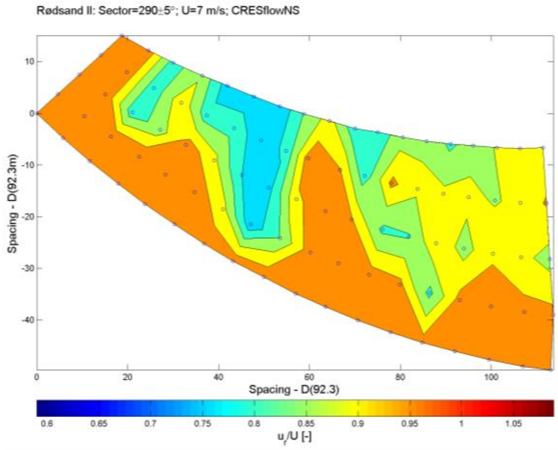

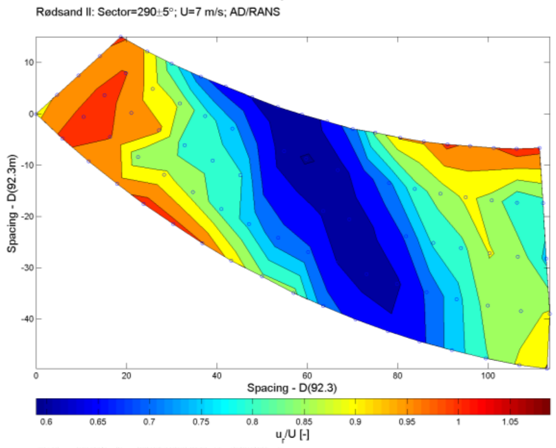

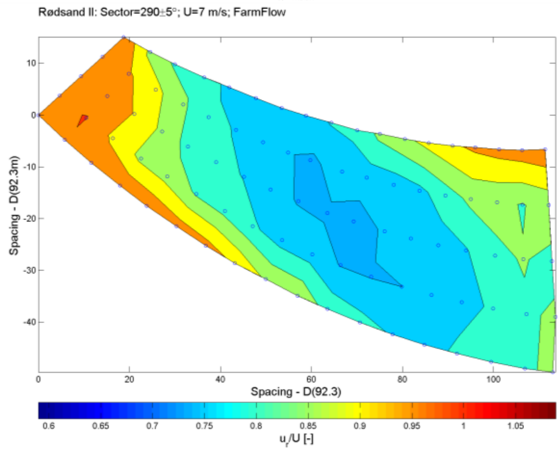

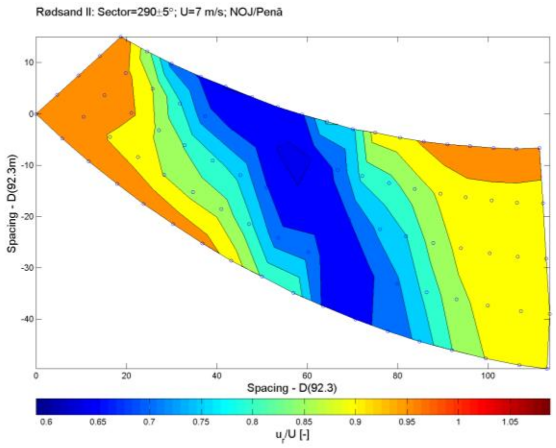

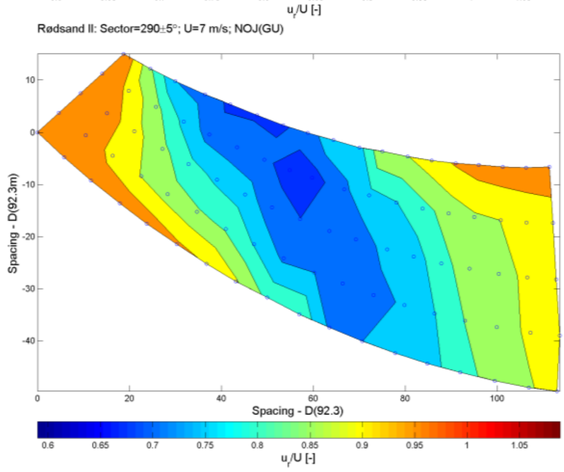

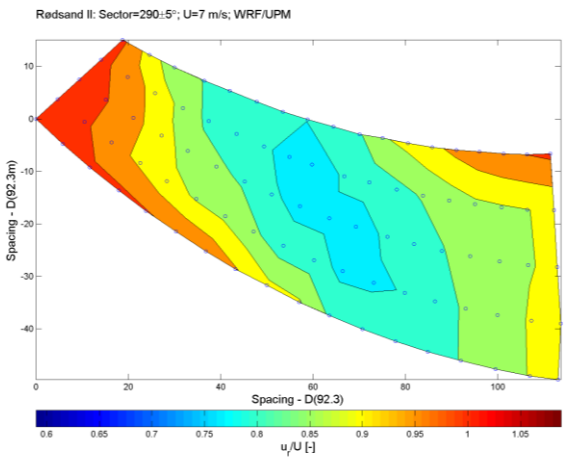

7.10 Power deficit along arch's, RS-290-7.

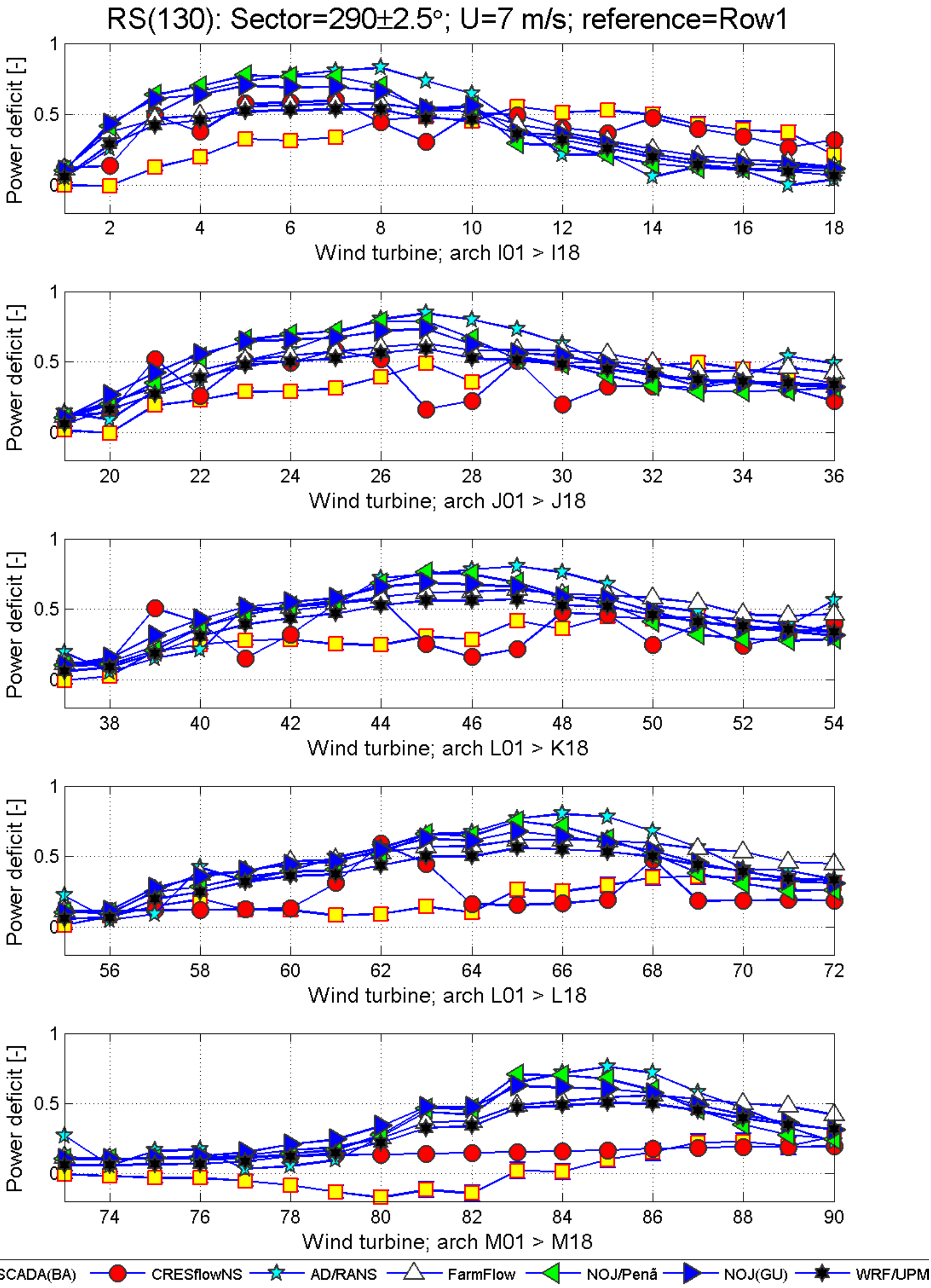

8 ANNEX B - EASTERN INFLOW DIRECTION

8.1 Case RS-77-8.

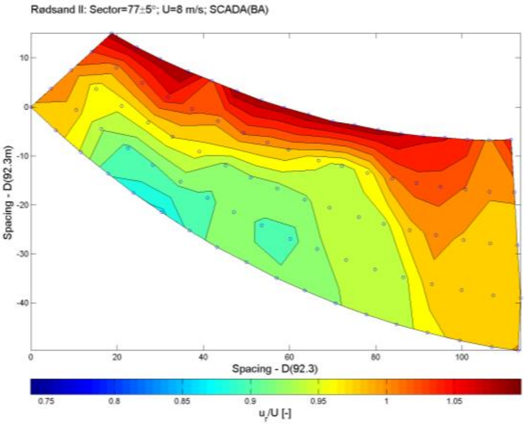

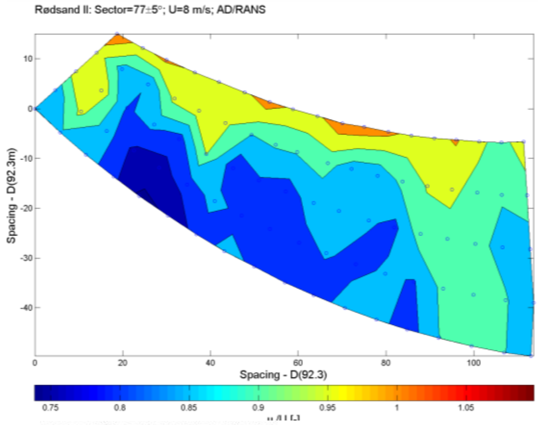

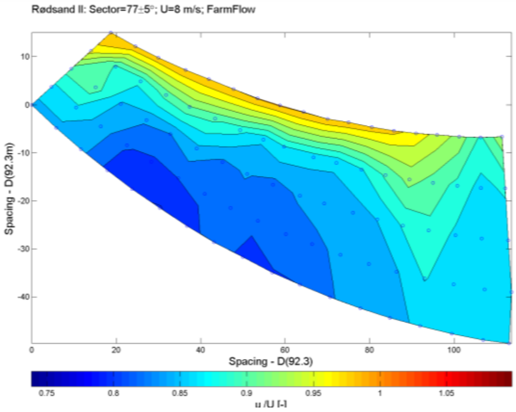

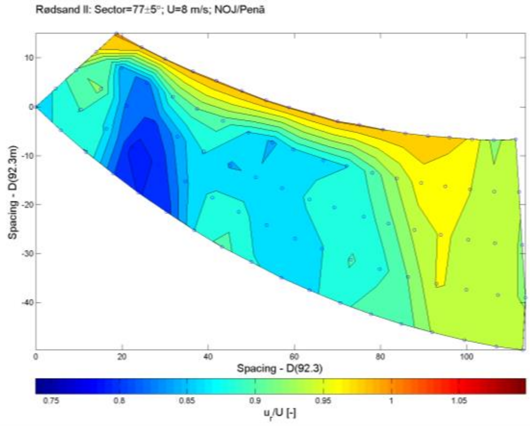

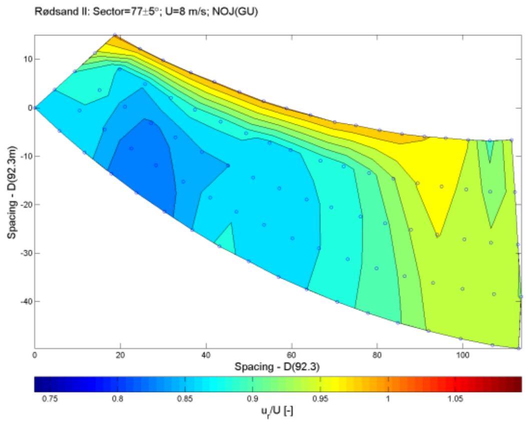

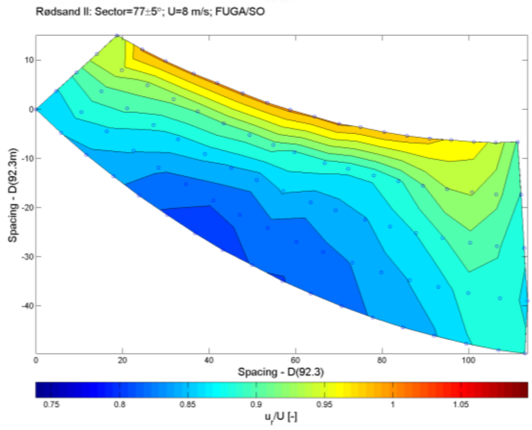

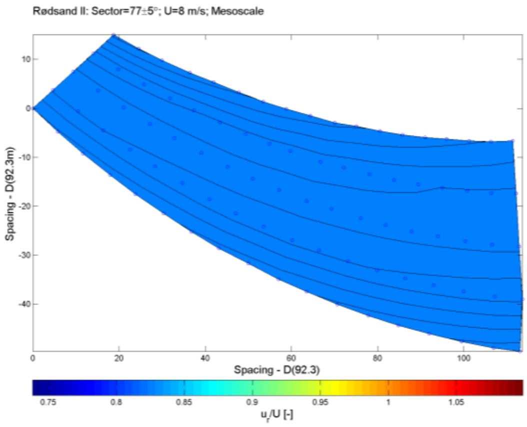

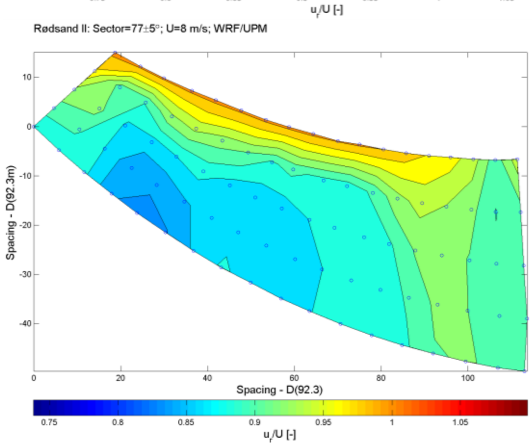

8.2 Power deficit along arch's, RS-77-8.

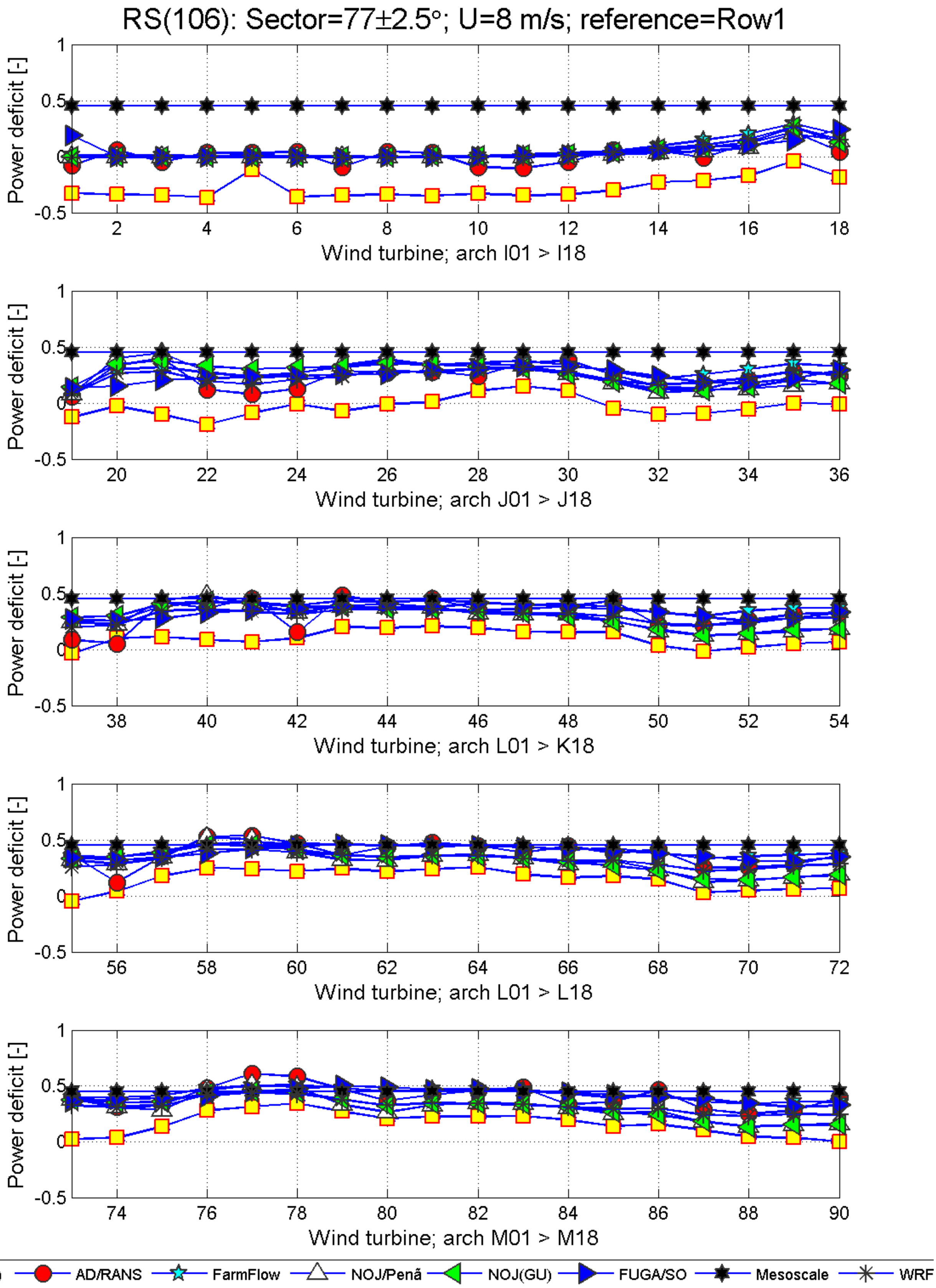

8.3 Case RS-87-8.

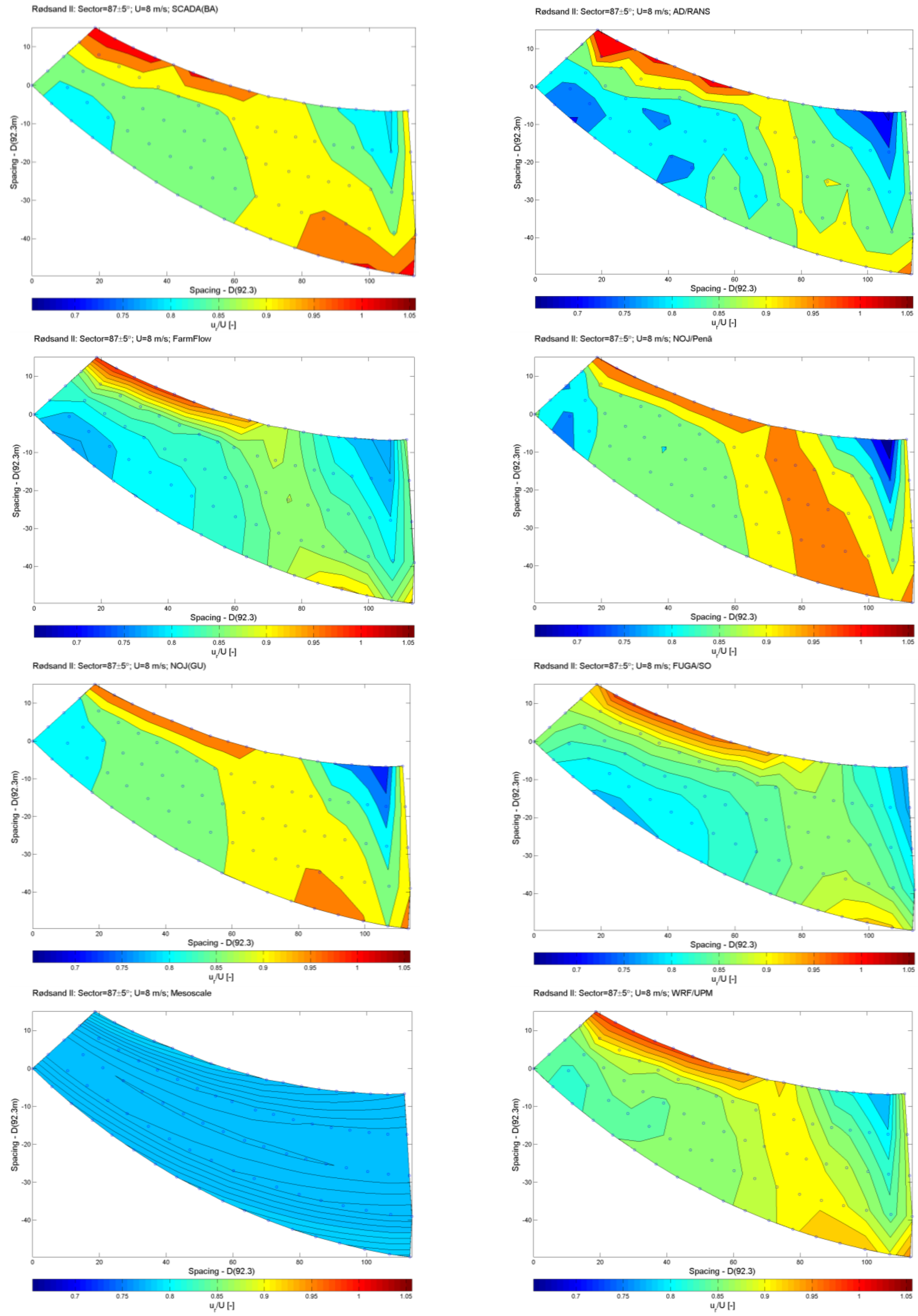

8.4 Power deficit along arch's, RS-87-8

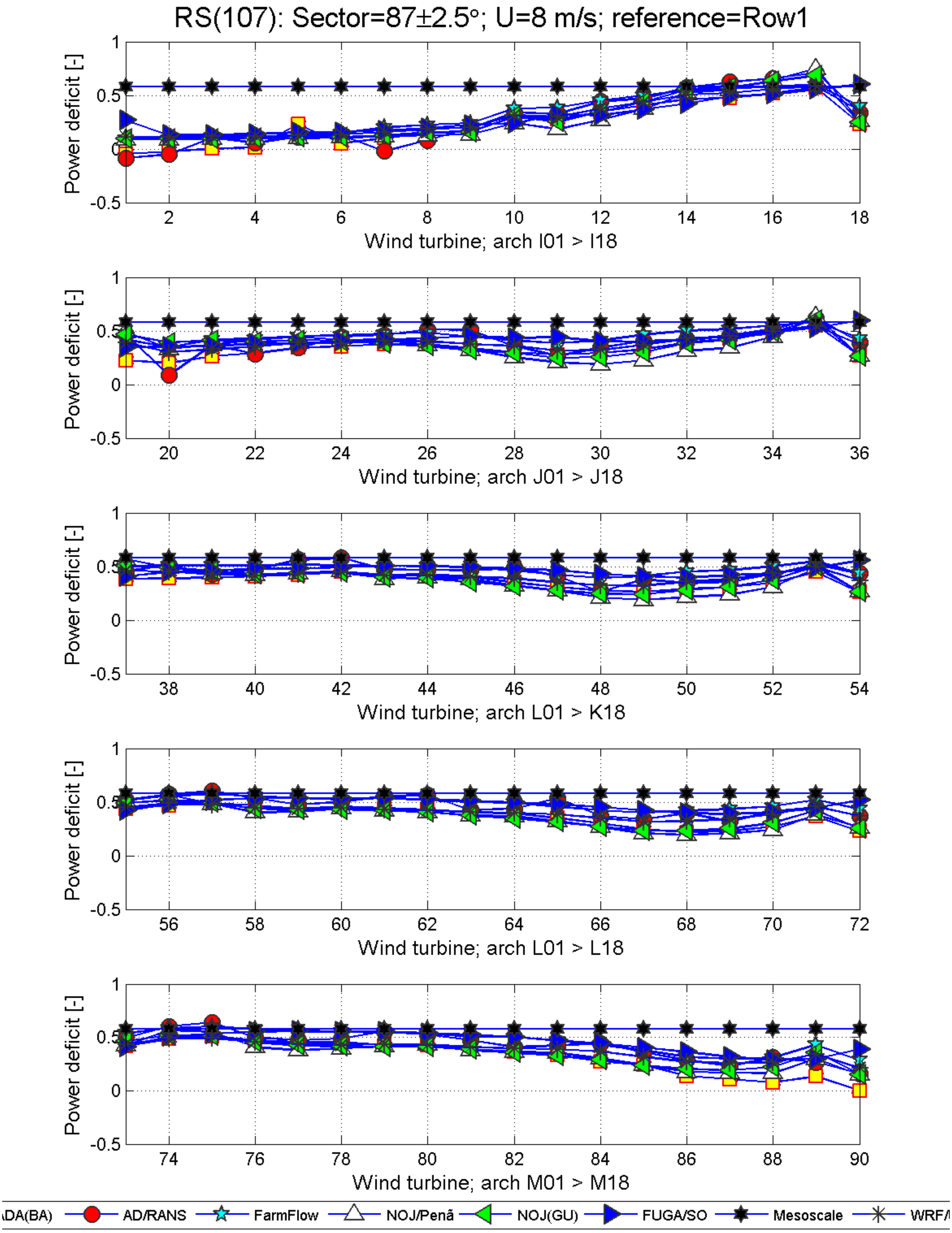

8.5 Case RS-97-8.

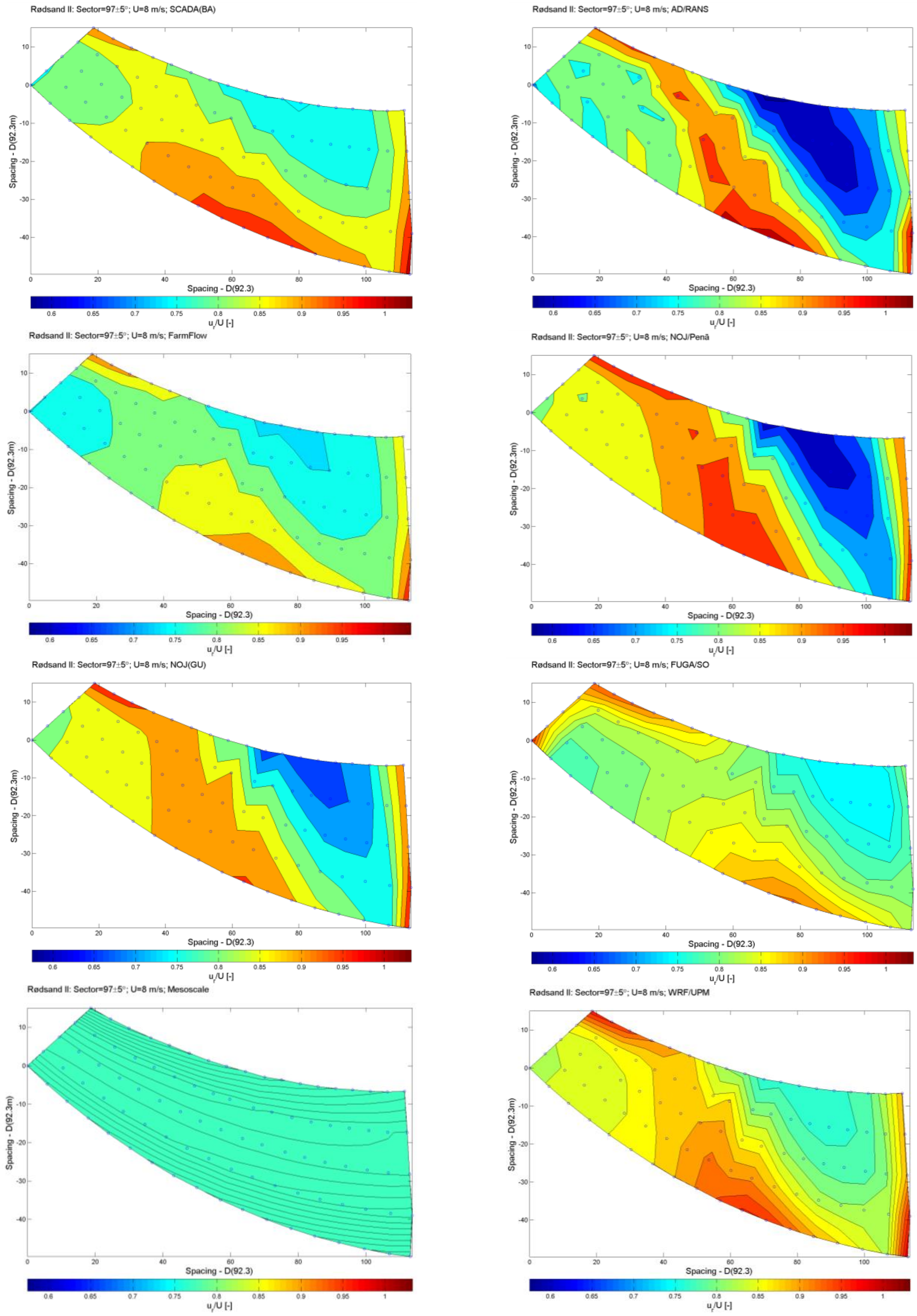

8.6 Power deficit along arch's, RS-97-8

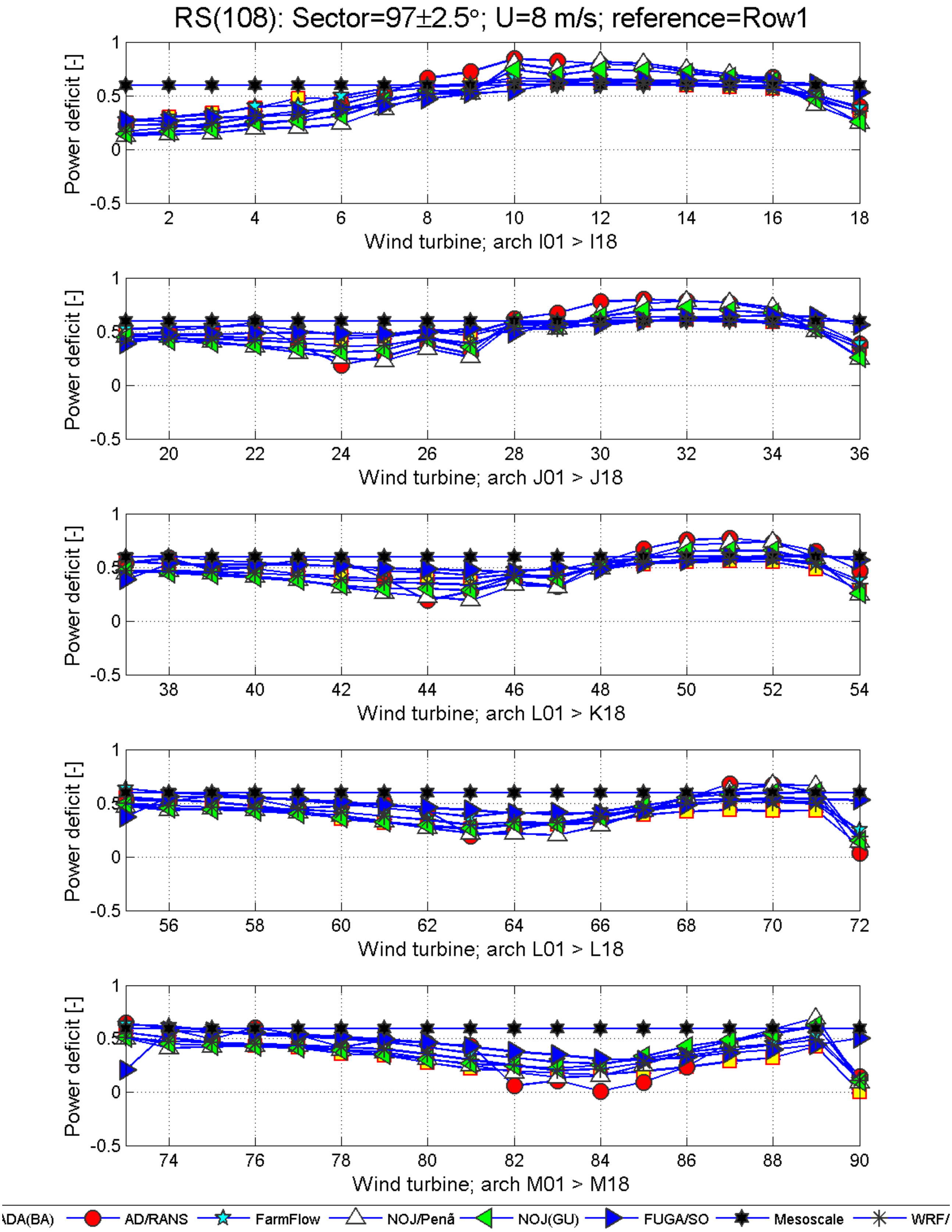

8.7 Case RS-107-8.

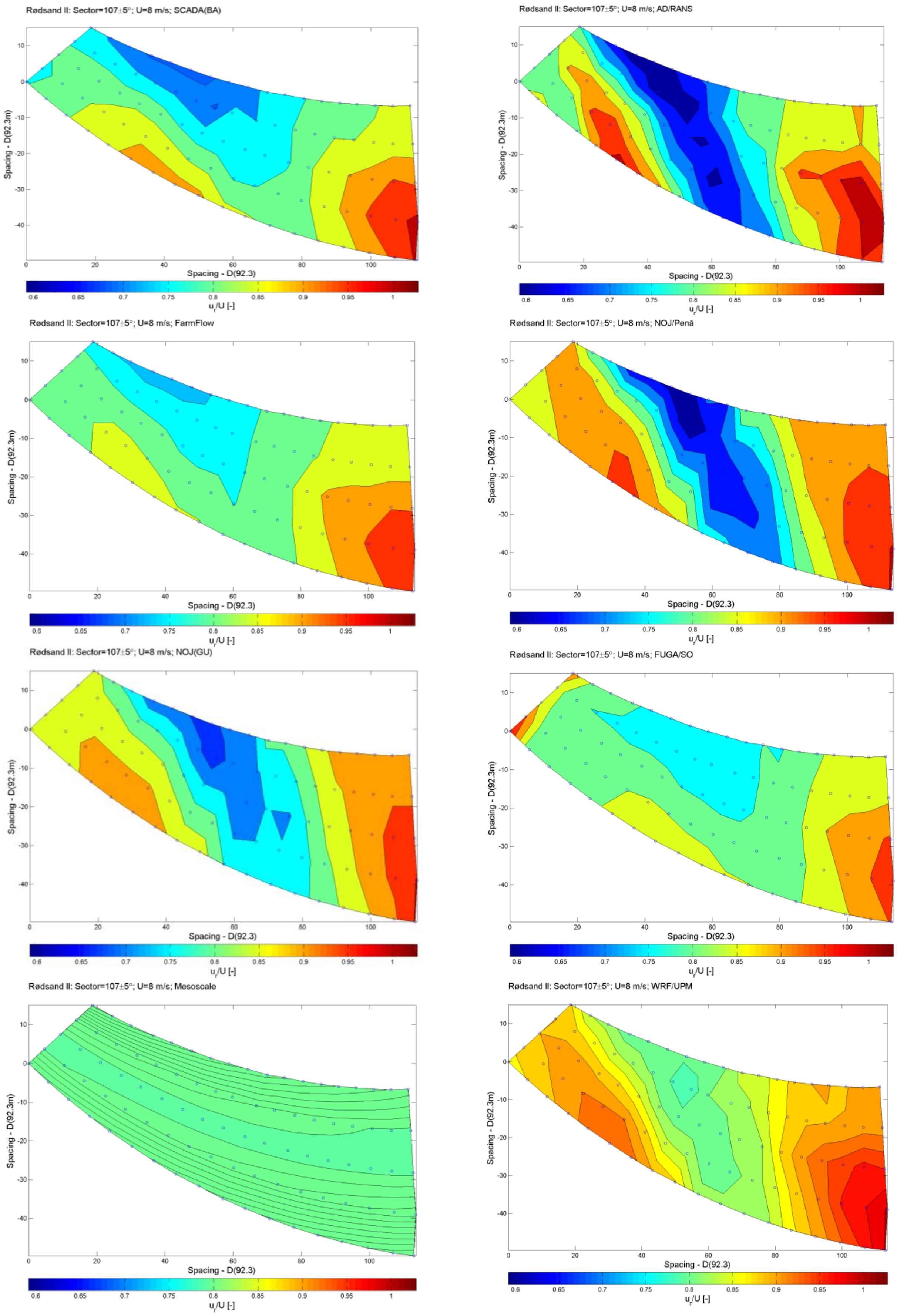

8.8 Power deficit along arch's, RS-107-8

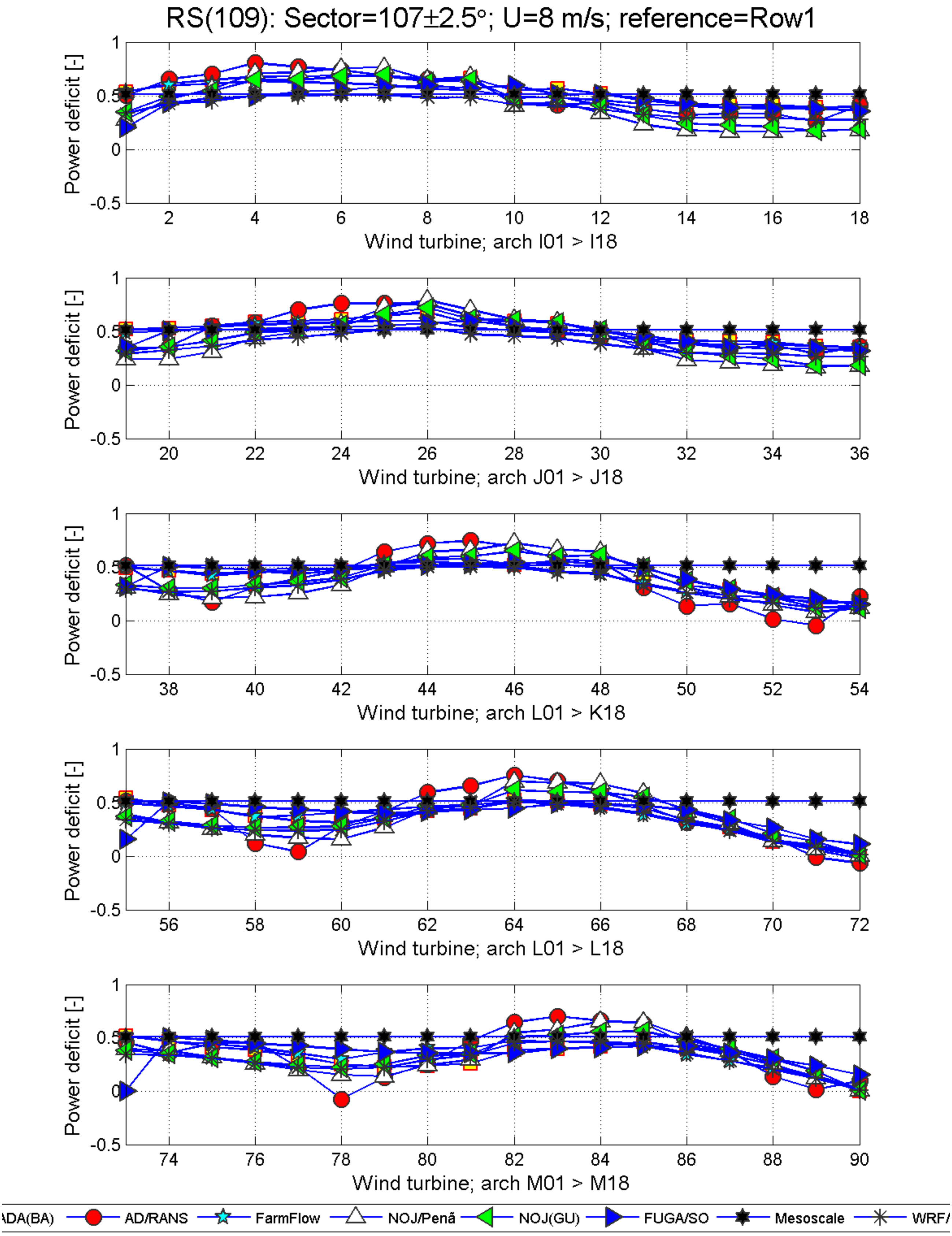

8.9 Case RS-117-8.

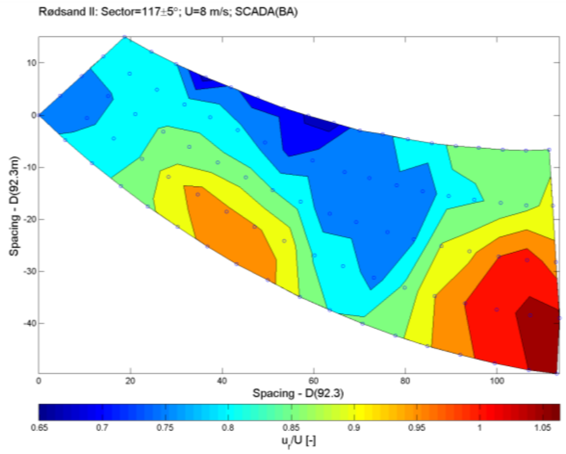

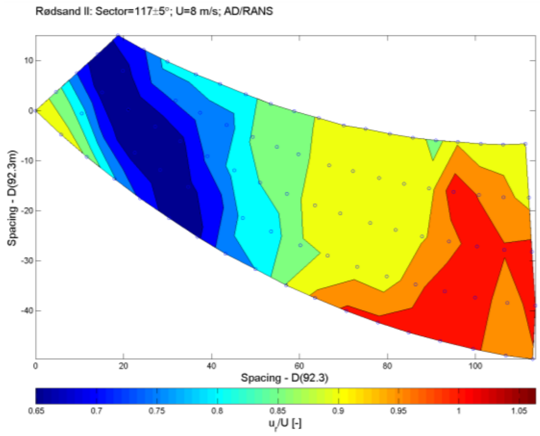

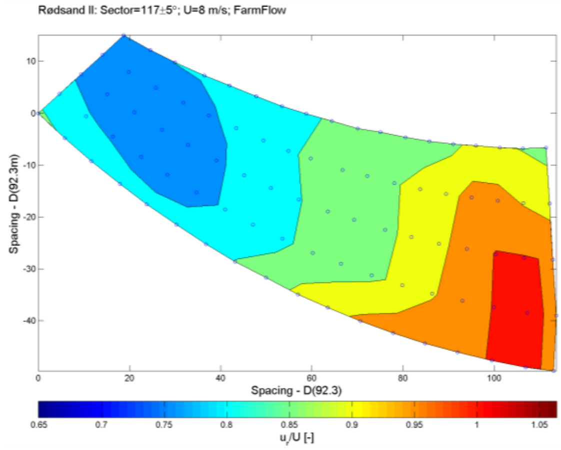

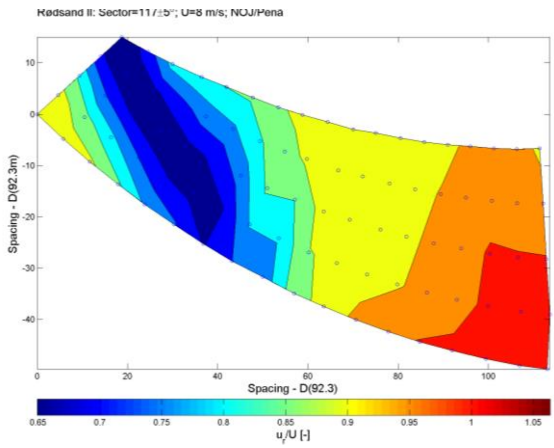

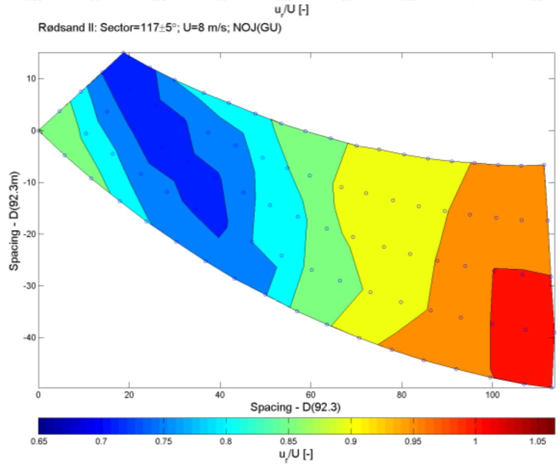

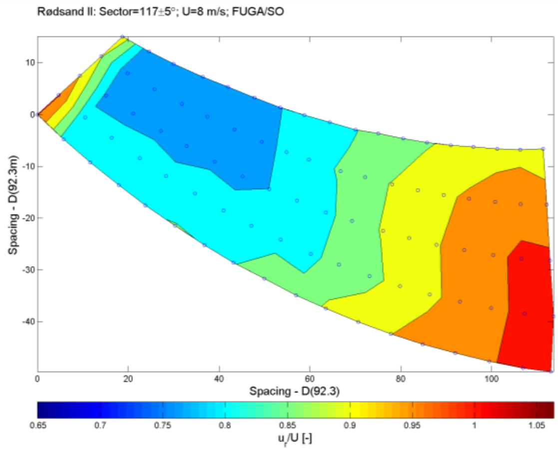

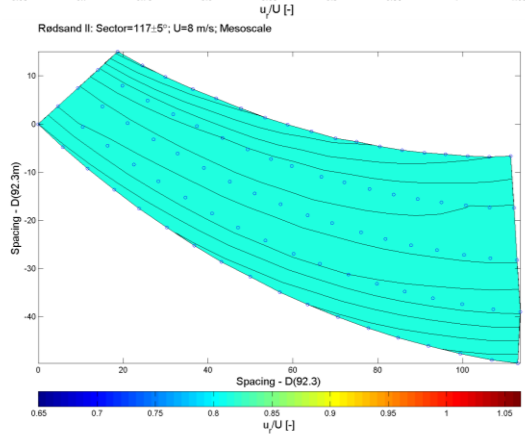

8.10 Power deficit along arch's, RS-117-8

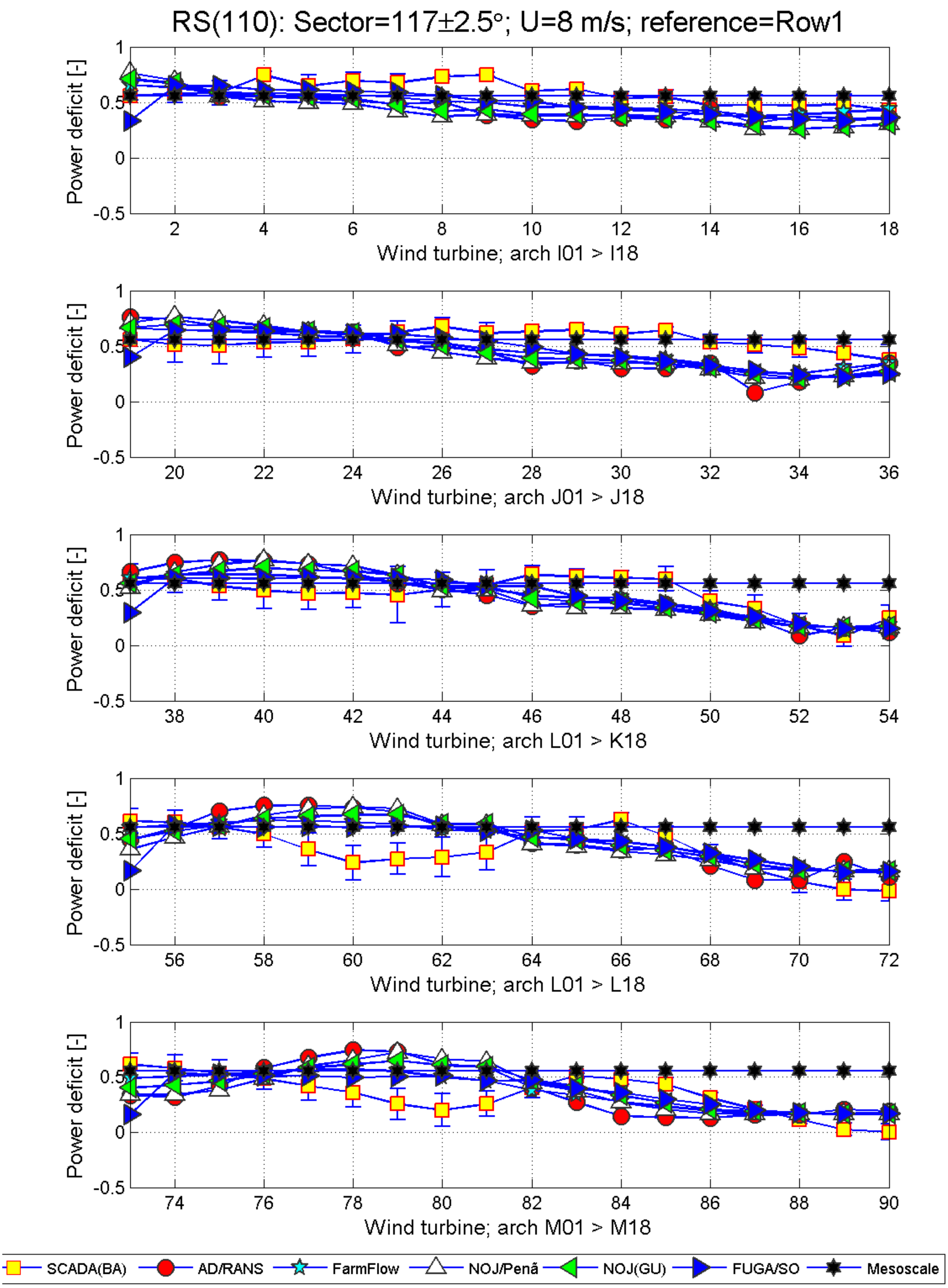

9 ANNEX C - CLUSTER EFFECT FOR EASTERLY INFLOW;

9.1 Case NY & RS-77-8

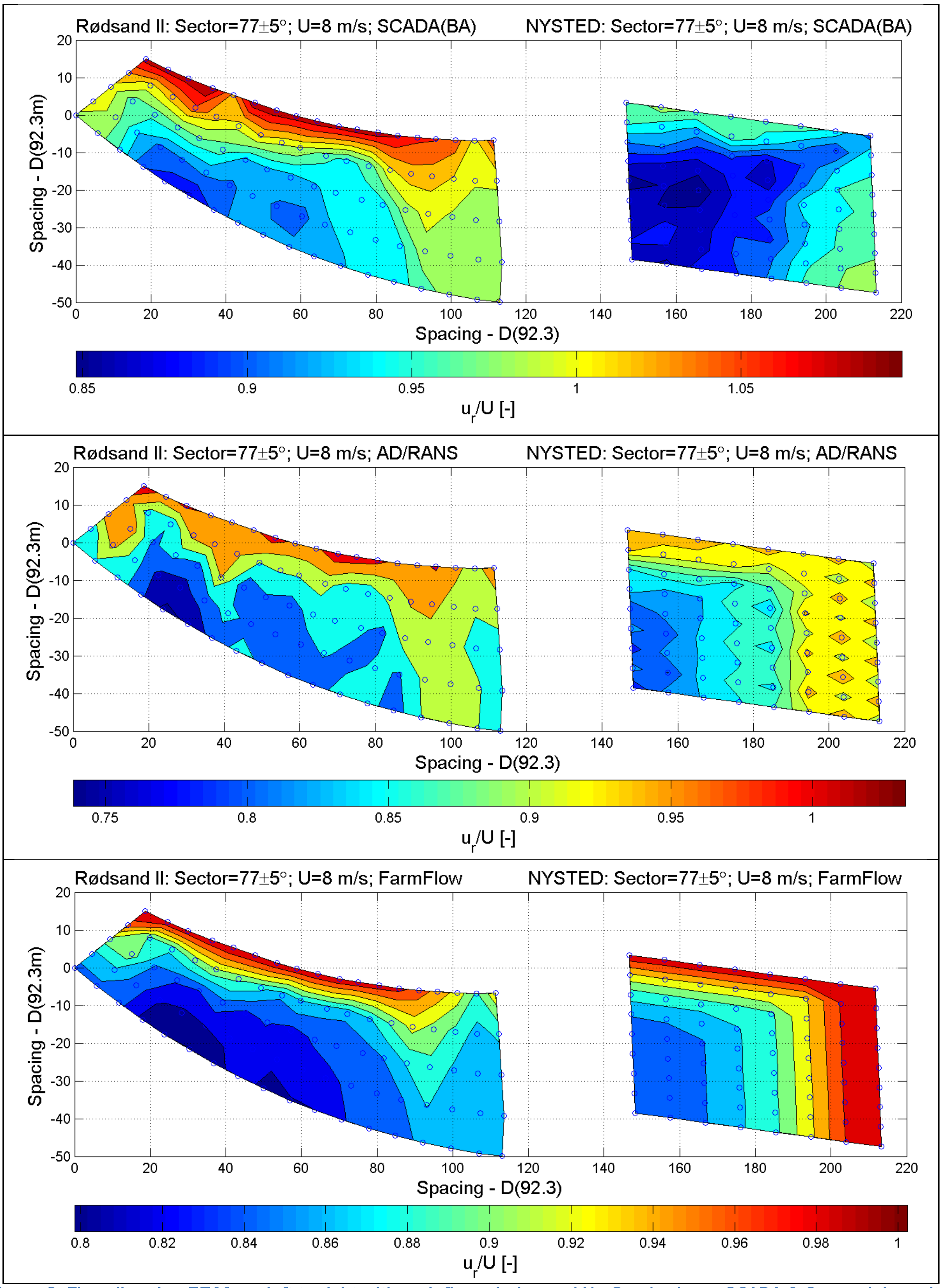

Figure 6: Flow direction 77° from left to right with an inflow wind speed U= 8 m/s shows SCADA & 2 x model results.

9.2 Case NY & RS-87-8

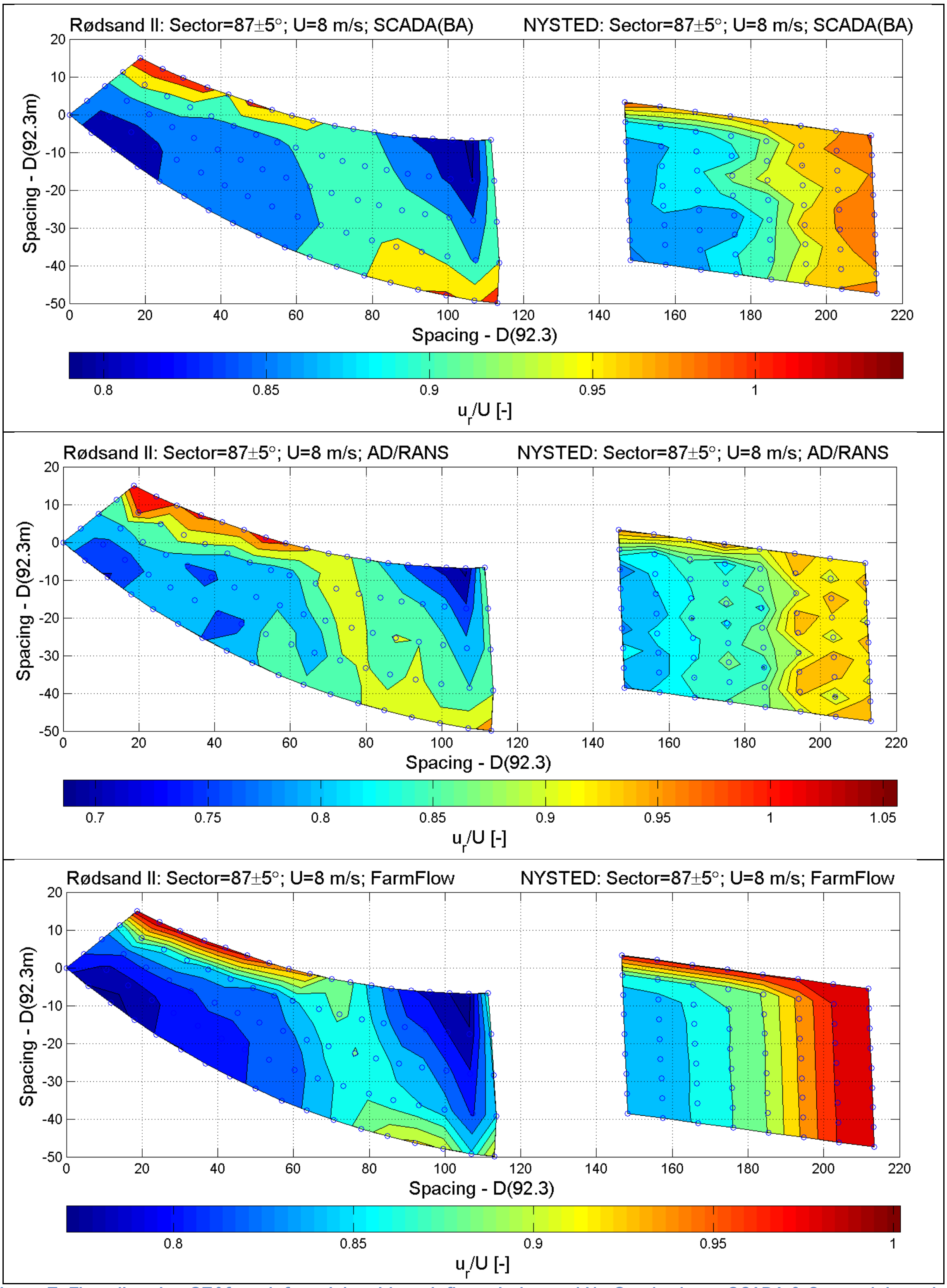

Figure 7: Flow direction 87° from left to right with an inflow wind speed U= 8 m/s shows SCADA & 2 x model results.

9.3 Case NY & RS-97-8

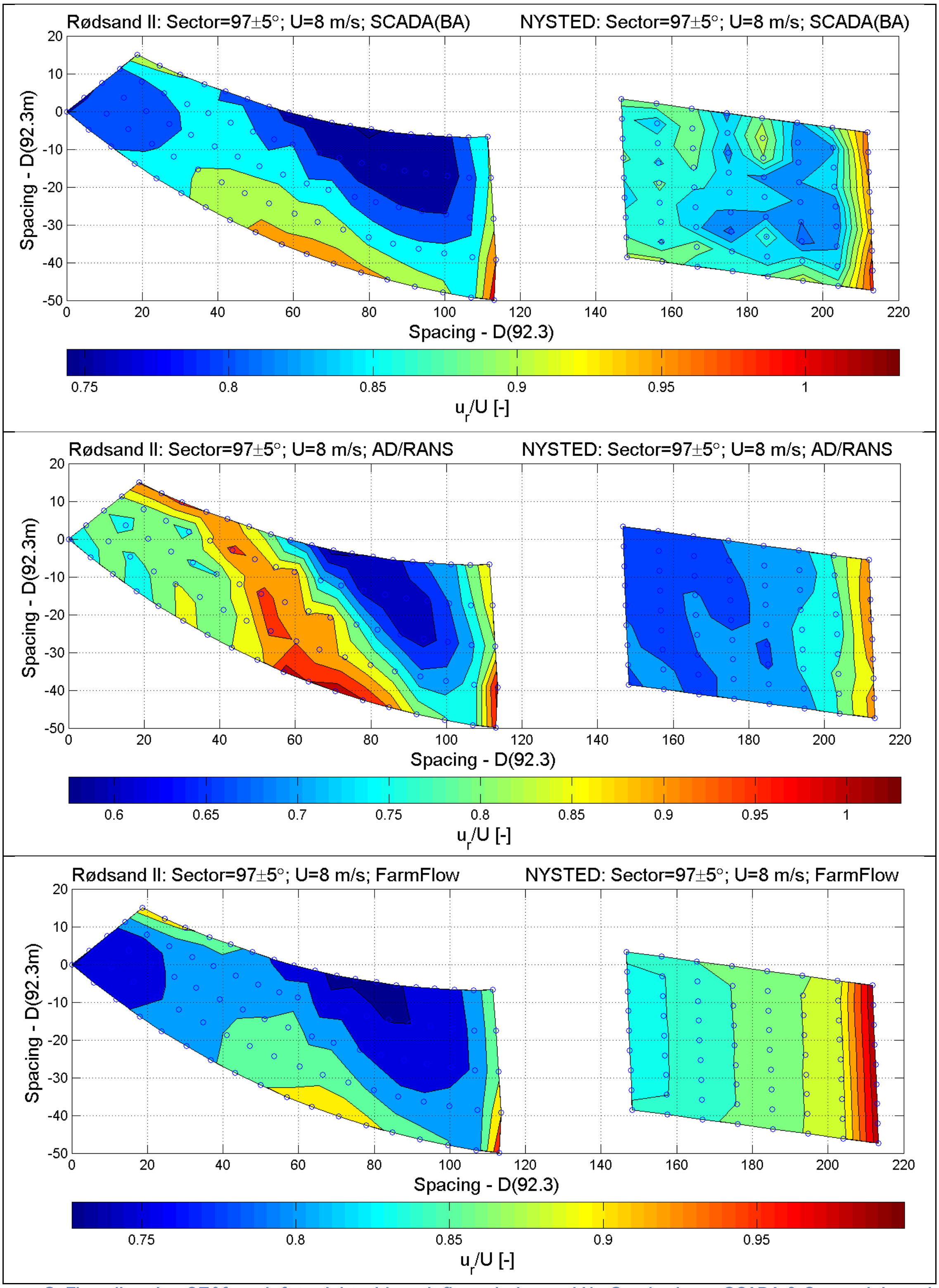

Figure 8: Flow direction 97° from left to right with an inflow wind speed U= 8 m/s shows SCADA & 2 x model results.

9.4 Case NY & RS-107-8

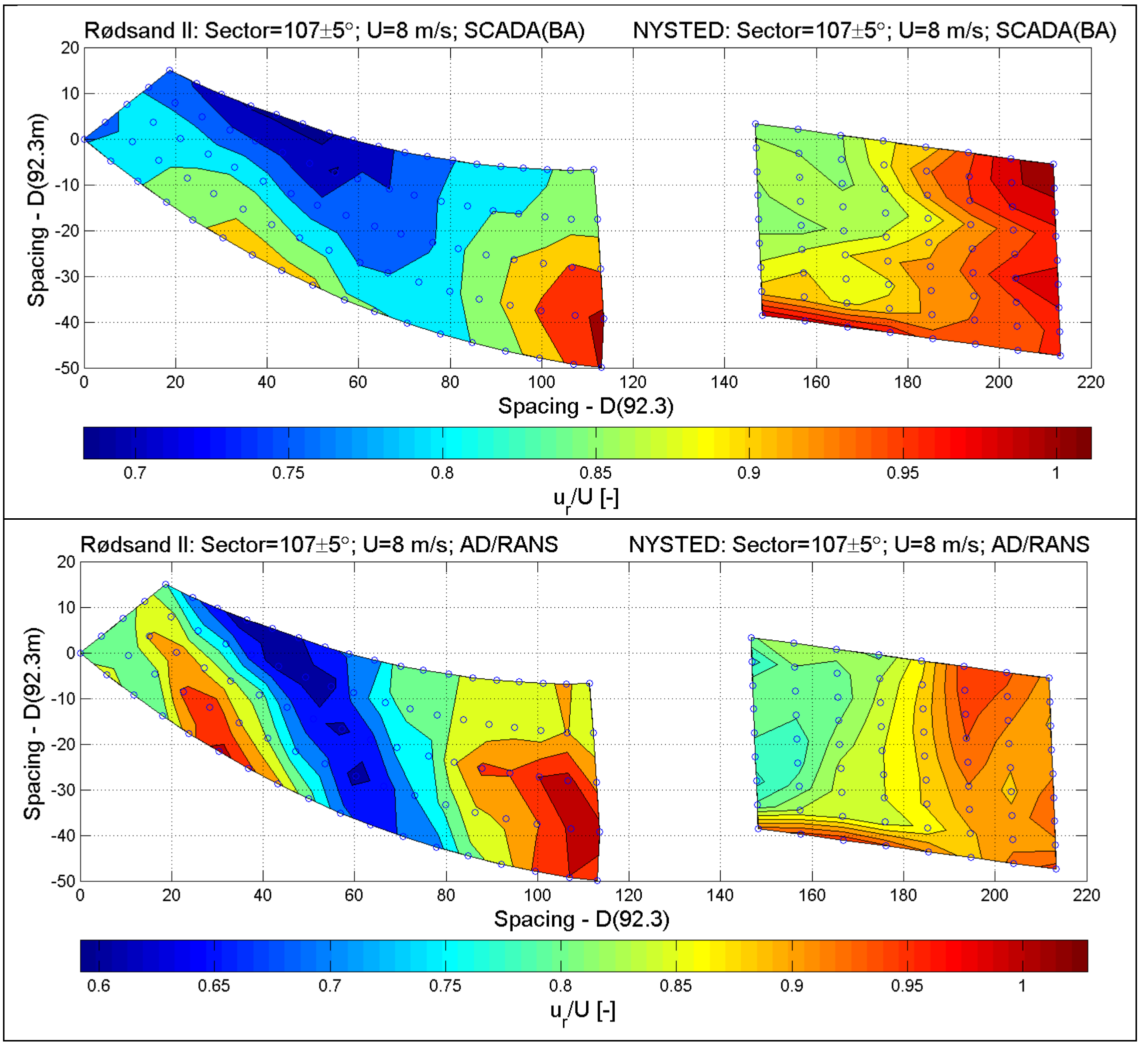

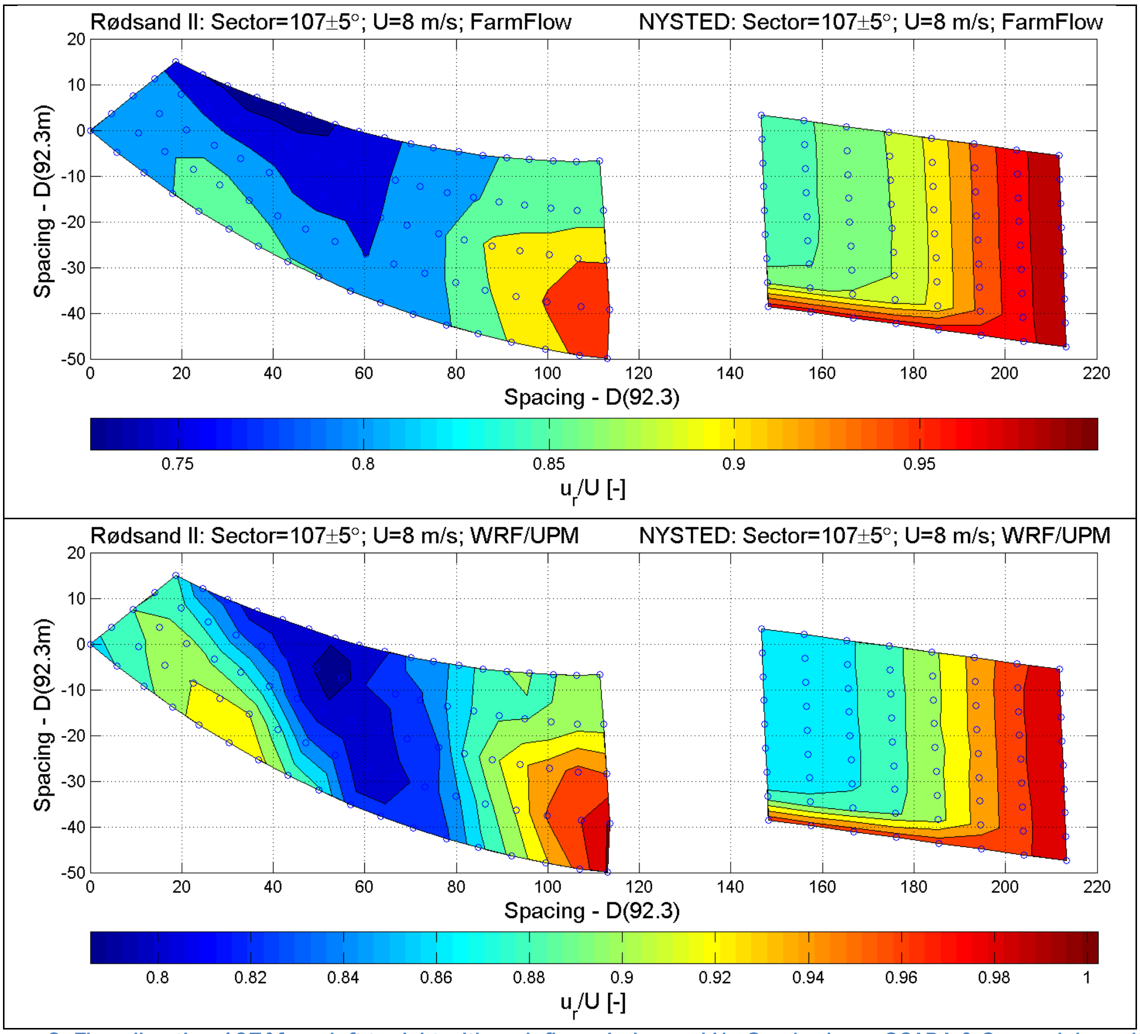

Figure 9: Flow direction 107° from left to right with an inflow wind speed U= 8 m/s shows SCADA & 3 x model results.

9.5 Case NY & RS-117-8

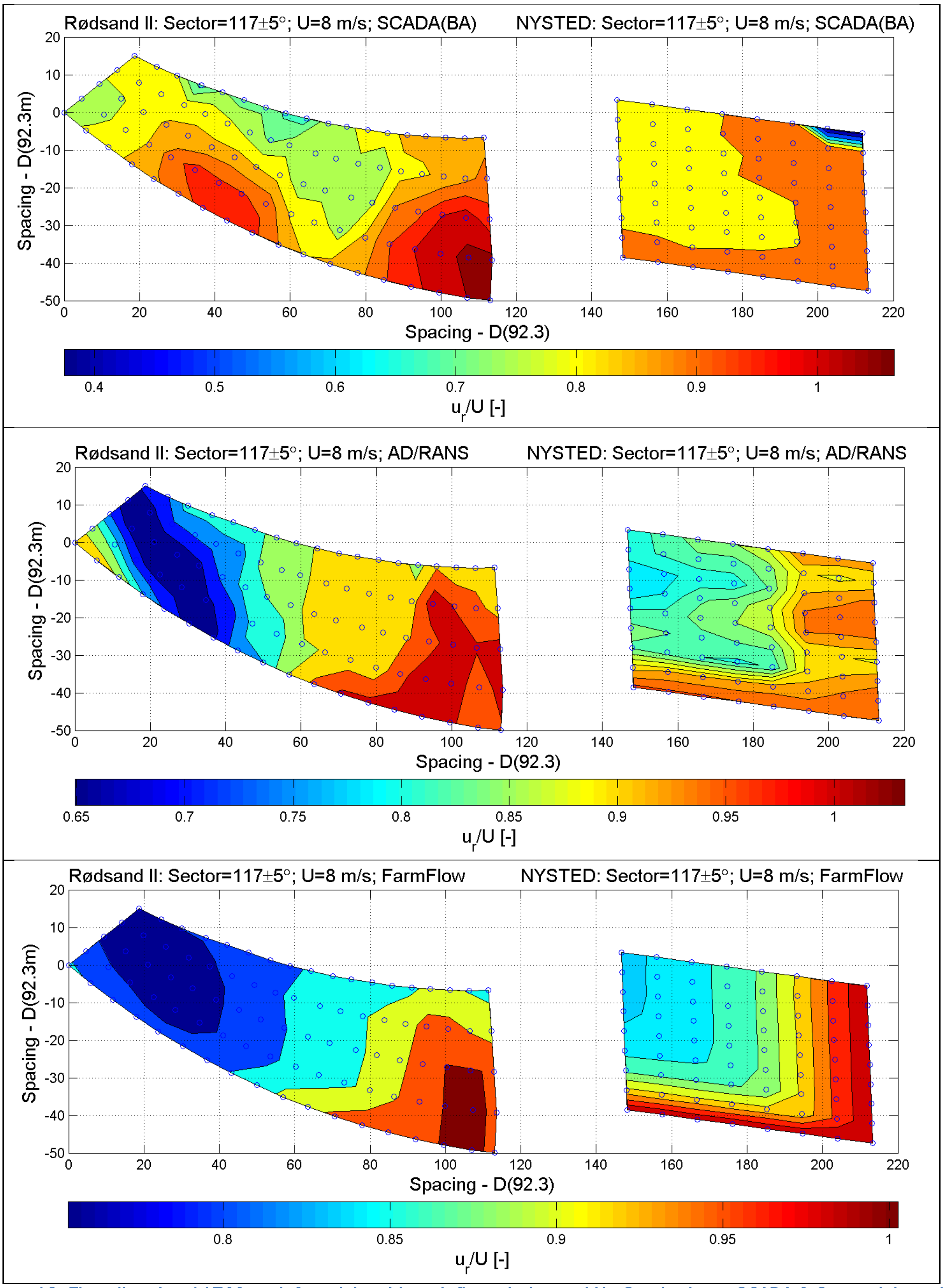

Figure 10: Flow direction 117° from left to right with an inflow wind speed U= 8 m/s shows SCADA & 2 x model results.